

**UNIVERSITY OF GAZIANTEP
GRADUATE SCHOOL OF
NATURAL & APPLIED SCIENCES**

**EXPRIMNETAL STUDY OF LOCAL SCOUR
DOWENSTREAM OF CYLINDRICAL
BRIDGE PIER**

**M.Sc. THESIS
IN
CIVIL ENGINEERING**

**BY
MOHAMMED TAREQ ALSHAREEF**

JANUARY 2013

**Experimental Study of Local Scour Downstream of
Cylindrical Bridge Pier**

**M.Sc. Thesis
in
Civil Engineering
University of Gaziantep**

**Supervisor
Prof. Dr. Mostafa GUNAL**

**by
Mohammed Tareq ALSHAREEF**

January 2013

©2013 [Mohammed Tareq ALSHAREEF]


T.C.
UNIVERSITY OF GAZİANTEP
GRADUATE SCHOOL OF
NATURAL & APPLIED SCIENCES
CIVIL ENGINEERING DEPARTMENT

Name of the thesis : Experimental Study of Local Scour Downstream of
Cylindrical Bridge Piers

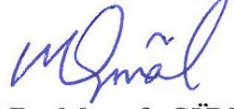
Name of the student : Mohammed Tareq AL-SHAREEF

Exam date : 23.01.2013


Approval of the Graduate School of Natural and Applied Sciences


Assoc. Prof. Dr. Metin BEDİR
Director

I certify that this thesis satisfies all the requirements as a thesis for the degree of
Master of Science.


Prof. Dr. Mustafa GÜNAL
Head of Department

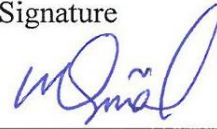
This is to certify that we have read this thesis and that in our opinion it is fully
adequate, in scope and quality, as a thesis for the degree of Master of Science.


Prof. Dr. Mustafa GÜNAL
Supervisor

Examining Committee Members

Signature

Prof. Dr. Mustafa GÜNAL



Assoc. Prof. Dr. Aytaç GÜVEN



Assist. Prof. Dr. Hüsnü UGUR



I hereby declare that all information in this document has been obtained and presented in accordance with academic rules and ethical conduct. I also declare that, as required by these rules and conduct, I have fully cited and referenced all material and results that are not original to this work.

Mohammed Tareq AL SHAREEF

Signature

ABSTRACT

EXPERIMENTAL STUDY OF LOCAL SCOUR DOWNSTREAM OF CYLINDRICAL BRIDGE PIERS

AL SHAREEF, MOHAMMED

M.Sc. in Civil Engineering

Supervisor: Prof. Dr. Mustafa GÜNAL

Co-supervisor: Assist. Prof. Dr. Hamid H. HUSSEIN

February 2013

84 Pages

Scour is a natural phenomenon caused due to the erosive action of flowing stream on alluvial beds which removes the sediment around or near structures located in flowing water. It means the lowering of the riverbed level by water erosions such that there is a tendency to expose the foundations of a structure. The failure of bridges piers are due to many reasons such as localized scour combined with general riverbed degradation. In this study we try to investigate the temporal variation of scour depth at uniform cylindrical bridge pier with different diameters. The experimental work is carried out in the hydraulic laboratory of civil engineering at Gaziantep University on a channel have dimensions of 8.3m length, 0.8m width and 0.9m depth. The experiments will be carried on 20 cm depth of sediment layer having $d_{50}=0.4$ mm. Three bridge pier shapes having different scaled models will be constructed in a 1.5m of test section in the channel. In this study, predicted maximum scour depth equation was found by using analysis program, depending on experimental data.

Keywords: scour, local scour, bridge piers, scour depth.

ÖZET

SİLİNDİRİK OLAN KÖPRÜ AYAK MANSABINDA OLUŞAN YEREL OYULMANIN DENEYSEL OLARAK İNCELENMESİ

AL SHAREEF, MOHAMMED

Yüksek Lisans Tezi, İnşaat Mühendisliği Bölümü

Tez Yöneticisi: Prof. Dr. Mustafa GÜNAL

Yardımcı Tez Yöneticisi: Assist. Prof. Dr. Hamid H. HUSSEIN

Ocak 2013

84 Sayfa

Suyun aşındırma etkisinden dolayı, suyun içerisine yapılmış olan yapıların etrafında veya yakınlarındaki alüvyon malzeme hareket eder ve bu olay yerel oyulma olarak adlandırılır. Yerel oyulma sonucunda nehir yatağı seviyesi düşer ve yapının temelini ortaya çıkarabilir. Nehir yatağının aşınmasıyla birlikte oluşan yerel oyulma sonucunda köprü ayakları yük taşıma özelliklerini kaybederler. Bu çalışmada farklı çaptaki silindirik köprü ayak mansabında oluşan yerel oyulma derinliğinin zamana göre değişimi deneysel olarak incelenmiştir. Deneysel Gaziantep Üniversitesi, hidrolik laboratuvarında bulunan 8.3m uzunluğunda, 0.8m genişliğinde ve 0.9m derinliğindeki açık kanalda yapılmıştır. Deneysel 20cm kalınlığında ve dane çapı $d_{50}=0.4$ mm olan kum üzerinde yapılmıştır. Üç farklı çaptaki köprü ayak modelleri kanal içerisinde 1.5m uzunluğundaki kum taban üzerinde yapılmıştır. Bu çalışmada, maksimum yerel oyulmayı tahmin eden denklem bir analiz programına deneysel elde edilen maksimum yerel oyulma derinlikleri girilerek bulunmuştur.

Anahtar Kelimeler: oyulma, yerel oyulma, köprü ayağı, oyulma derinliği.

*This thesis is dedicated to my beloved Dad, Mom, My Brothers and
Sister for their endless love, support and encouragement*

ACKNOWLEDGEMENTS

First praise is to Allah, the Almighty, on whom ultimately we depend for sustenance and guidance. Secondly I offer my sincerest gratitude to my supervisor, Prof. Dr. Mustafa GUNAL, whose encouragement, guidance and support from the initial to the final level enabled me to understand and work for the development of the subject.

I would like to thank my parents for their support and great patience at all times. My brothers, sister and have given me their unequivocal support throughout, as always, for which my mere expression of thanks likewise does not suffice.

Finally, I would like to thank all those helped to reach the successful realization of thesis, as well as expressing my apology for not mentioning them all.

TABLE OF CONTENTS

CONTENT	Page
ABSTRACT.....	v
ÖZET.....	vi
ACKNOWLEDGMENTS.....	viii
CONTENTS.....	ix
LIST OF FIGURES	xii
LIST OF TABLES.....	xiv
LIST OF SYMBOLS.....	xv
CHAPTER 1: INTRODUCTION.....	1
1.1 General.....	1
1.2 Local Scour.....	2
1.3 Mechanism of Local Scour.....	3
1.4 Objective of Study.....	5
1.5 Layout of thesis.....	5
CHAPTER 2: LITERATURE REVIEW.....	7
2.1 Introduction.....	7
2.2 Physical Modeling of Local Scour Around Bridge Pier.....	7
2.3 Scour Prediction Equation.....	11
2.4 Parameter Affecting on local scour.....	15
2.4.1 Pier Geometry.....	15
2.4.2 Sediment Coarseness and Gradation.....	16
2.4.3 Temporal Development of Scour.....	18
2.4.4 Flow Intensity.....	20
2.4.5 Pier Size.....	21
2.4.6 Flow Depth.....	21
CHAPTER 3: EXPERIMENTAL STUDY AND METHODOLOGY.....	23
3.1 Introduction.....	23
3.2 Experimental Flume.....	23

3.3 Bridge Pier Models.....	25
3.4 Sand Bed.....	26
3.5 Experimental Methodology.....	27
3.5.1 Program of The Work.....	27
3.5.2 Experimental Procedure.....	28
CHAPTER 4: RESULTS AND DESCUSSION.....	31
4.1 Introduction.....	31
4.2 Local Scour Depth.....	31
4.2.1 Measurement of Local Scour Depth With $d=5\text{cm}$ and $Q=6.29\text{ lt/s}$	31
4.2.2 Measurement of Local Scour Depth With $d=5\text{cm}$ and $Q=6.16\text{ lt/s}$	32
4.2.3 Measurement of Local Scour Depth With $d=5\text{cm}$ and $Q=22.63\text{ lt/s}$	34
4.2.4 Measurement of Local Scour Depth With $d=5\text{cm}$ and $Q=25.19\text{ lt/s}$	35
4.2.5 Bathymetry and 3-dimensional view of the scoured bed for Group 1 tests...	37
4.3 Local Scour Depth.....	41
4.3.1 Measurement of Local Scour Depth With $d=7.5\text{cm}$ and $Q=6.29\text{ lt/s}$	42
4.3.2 Measurement of Local Scour Depth With $d=7.5\text{cm}$ and $Q=6.16\text{ lt/s}$	42
4.3.3 Measurement of Local Scour Depth With $d=7.5\text{cm}$ and $Q=22.63\text{ lt/s}$	44
4.3.4 Measurement of Local Scour Depth With $d=7.5\text{cm}$ and $Q=25.19\text{ lt/s}$	46
4.3.5 Bathymetry and 3-dimensional View of the scoured bed for Group 2 tests..	47
4.3.6 Comparison Between Group1 and Group 2 Results.....	52
4.3.7 Longitudinal Scour Profile for Group 2 Tests.....	52
4.4 Local Scour Depth.....	54
4.4.1 Measurement of Local Scour Depth With $d=11.1\text{cm}$ and $Q=6.29\text{ lt/s}$	54
4.4.2 Measurement of Local Scour Depth With $d=11.1\text{cm}$ and $Q=6.16\text{ lt/s}$	55
4.4.3 Measurement of Local Scour Depth With $d=11.1\text{cm}$ and $Q=22.63\text{ lt/s}$	57
4.4.4 Measurement of Local Scour Depth With $d=11.1\text{cm}$ and $Q=25.19\text{ lt/s}$	58
4.4.5 Bathymetry and 3-dimensional view of the scoured bed for Group 3 tests..	60
4.4.6 Comparison Between Group2 and Group 3 Results.....	65
4.4.7 Longitudinal Scour Profile for Group 3 Tests.....	65
4.5 Predicted Maximum Scour Depth.....	67
4.5.1 Linear Regression Method.....	68
4.5.2 Linear + Interaction Method.....	69
4.5.3 Quadratic Regression Method.....	70
CHAPTER 5: CONCLUSIONS.....	73
5.1 Conclusion.....	73

5.2 Recommendation for future study.....	74
REFERENCES.....	74
APPENDIX A: Data for scour profile.....	79
APPENDIX B: Input Data for Step-Wise Regression.....	84

LIST OF FIGURES

Figure 1.1. Time-dependent development of scour depth.....	4
Figure 1.2. Flow and scour pattern at a circular pier.....	5
Figure 2.1. Schematic diagram of the three different phases of the scour process...	20
Figure 3.1. General View of the Laboratory Flume.....	23
Figure 3.2. General View of the Bridge Pier.....	23
Figure 3.3. Schematic illustration of the experimental flume system.....	24
Figure 3.4. Pier model.....	25
Figure 3.5. Sand specific gravity field test.....	26
Figure 3.6. Grain size distributions (sieve analysis).....	27
Figure 3.7. Experimental setup.....	28
Figure 4.1. Time evolution in scour depth for $d= 5\text{cm}$, $Q=6.29\text{ lt/s}$	32
Figure 4.2. Time evolution in scour depth for $d= 5\text{cm}$, $Q=16.6\text{ lt/s}$	33
Figure 4.3. Time evolution in scour depth for $d= 5\text{cm}$, $Q=22.63\text{ lt/s}$	35
Figure 4.4. Time evolution in scour depth for $d= 5\text{cm}$, $Q=25.19\text{ lt/s}$	36
Figure 4.5. Time evolution in scour depth for all test in Group 1.....	37
Figure 4.6. 3D scour map for SA1.....	38
Figure 4.7. 3D scour map for SA2.....	38
Figure 4.8. 3D scour map for SA3.....	39
Figure 4.9. 3D scour map for SA4.....	39
Figure 4.10. Bathymetry of bed for Group1 tests.....	40
Figure 4.11. Equilibrium scour depth for Group 1 tests, $d=5\text{ cm}$	41
Figure 4.12. Time evolution in scour depth for $d= 7.5\text{cm}$, $Q=6.29\text{ lt/s}$	43
Figure 4.13. Time evolution in scour depth for $d= 7.5\text{cm}$, $Q=16.6\text{ lt/s}$	44
Figure 4.14. Time evolution in scour depth for $d= 7.5\text{cm}$, $Q= 22.63\text{ lt/s}$	45
Figure 4.15. Time evolution in scour depth for $d=7.5\text{cm}$, $Q= 25.19\text{ lt/s}$	47
Figure 4.16. Time evolution in scour depth for all test in Group2.....	48
Figure 4.17. Equilibrium scour depth for group 2 tests ($d=7.5\text{cm}$).....	48
Figure 4.18. 3D scour map for SB1.....	49
Figure 4.19. 3D scour map for SB2.....	49

Figure 4.20. 3D scour map for SB3.....	50
Figure 4.21. 3D scour map for SB4.....	50
Figure 4.22. Bathymetry of the bed for Group 2 tests.....	51
Figure 4.23. Comparison of the temporal development of maximum scour depth between Group 1 and Group 2 tests.....	53
Figure 4.24. Longitudinal scour profile for Group 2 tests.....	53
Figure 4.25. Time evolution in scour depth for $d=11.1\text{cm}$, $Q= 6.29\text{ lt/s}$	55
Figure 4.26. Time evolution in scour depth for $d=11.1\text{cm}$, $Q= 16.6\text{ lt/s}$	56
Figure 4.27. Time evolution in scour depth for $d=11.1\text{cm}$, $Q= 23.26\text{ lt/s}$	58
Figure 4.28. Time evolution in scour depth for $d=11.1\text{cm}$, $Q= 25.19\text{ lt/s}$	59
Figure 4.29. Temporal variation of scour depth in SA4, SB4, and SC4 tests.....	60
Figure 4.30. Experimental work show pier for group 3 ($d=11.1\text{cm}$).....	61
Figure 4.31. 3D scour map for SC1.....	62
Figure 4.32. 3D scour map for SC2.....	62
Figure 4.33. 3D scour map for SC3.....	63
Figure 4.34. 3D scour map for SC4.....	63
Figure 4.35. Bathymetry of the bed for Group 3 tests.....	64
Figure 4.36. Comparison of the temporal development of maximum scour depth between Group 2 and Group 3.....	66
Figure 4.37. Longitudinal scour profile for Group 3.....	66
Figure 4.38. Step-wise regression input window.....	67
Figure 4.39. Comparing between determined and observed scour depth for linear equation.....	68
Figure 4.40. Comparing between determined and observed scour depth for linear+interaction equation.....	70
Figure 4.41. Comparing between determined and observed scour depth for quadratic equation.....	71

LIST OF TABLES

Table 2.1. Coefficient for pier alignment for the HEC-18 Equations.....	13
Table 2.2. Bed-condition correction factor (K_3) for the HEC-18 Equation.....	14
Table 2.3. Summary of predicted equilibrium scour depth equations.....	15
Table 2.4. Coefficient of pier shape.....	17
Table 2.5. Classification of local scour depending on D and y_o at bridge pier foundations.....	22
Table 3.1. Experimental conditions.....	30
Table 4.1. Temporal development of scour depth for SA1($d = 5\text{cm}, Q = 6.29\text{ lt/s}$)..	32
Table 4.2. Temporal development of scour depth for SA2($d = 5\text{cm}, Q = 16.6\text{ lt/s}$)...	33
Table 4.3. Temporal development of scour depth for SA3($d = 5\text{cm}, Q = 16.6\text{ lt/s}$)...	34
Table 4.4. Temporal development of scour depth for SA4($d = 5\text{cm}, Q = 16.6\text{ lt/s}$)...	35
Table 4.5. Temporal development of scour depth for SB1($d = 7.5\text{cm}, Q = 6.29\text{ lt/s}$)..	42
Table 4.6. Temporal development of scour depth for SB2($d = 7.5\text{cm}, Q = 16.6\text{ lt/s}$)..	43
Table 4.7. Temporal development of scour depth for SB3($d = 7.5\text{cm}, Q = 23.26\text{ lt/s}$)..	45
Table 4.8. Temporal development of scour depth for SB3($d = 7.5\text{cm}, Q = 25.19\text{ lt/s}$)..	46
Table 4.9. Temporal development of scour depth for SC1($d = 11.1\text{cm}, Q = 6.29\text{ lt/s}$)..	54
Table 4.10. Temporal development of scour depth for SC2($d = 11.1\text{cm}, Q = 16.6\text{ lt/s}$)..	56
Table 4.11. Temporal development of scour depth for SC3($d = 11.1\text{cm}, Q = 23.26\text{ lt/s}$)..	57
Table 4.12. Temporal development of scour depth for SC4($d = 11.1\text{cm}, Q = 25.19\text{ lt/s}$)..	59
Table 4.13. Summary of linear method.....	68
Table 4.14. Summary of linear+ interaction method.....	69
Table 4.15. Summary of quadratic method.....	71
Table 4.16. Comparison of three regression methods.....	72

LIST OF SYMBOLS

h	Depth of water flow (m)
Q	Approach discharge (lt/s)
d	Pier width (cm)
d_s	Local scour depth (m)
d_{se}	Equilibrium scour depth (m)
b_p	Width of the pier (cm)
u	Stream velocity (m^2/s)
u_{cr}	Critical velocity (m^2/s)
d_{50}	Median size of the sediment particle (mm)
d_{84}	Grain size for which 84% by weight of the sediment is finer (mm)
d_{16}	Grain size for which 16% by weight of the sediment is finer (mm)
Fr	Froude number
R	Reynolds number
R_b	Pier Reynolds number
σ_g	Geometric standard deviation of the sand size
t	Time (sec)
u^*	Shear velocity (m/s)
u^*c	Critical Shear velocity (m/s)
G_s	Specific Gravity of sand

CHAPTER 1

INTRODUCTION

1.1 General

Scour is defined as the erosion of streambed sediment around an obstruction in a flow field (Chang 1988). Its mean removal and movement the sand around piers or abutments or any structure in river bed. (It is the result of the erosive action of flowing water, excavating and carrying away material from the bed and banks of streams and from around the piers and abutments of bridges) (Richardson et al., 2001). According to statistic, 60% of all bridge failures result from scour and other hydraulic related causes and many lives' loss especially during flood seasons. The lowering in sediment level around pier or any structure called scour depth and there is many research to estimate depth of scour we trying in this study to estimate depth of scour in front of pier with different diameter. Depend on flow conditions scour can classified into two categories clear-water scour and live-bed scour. Clear-water scour occurs when there is fluid-structure interaction. In this case the stream velocity (u) of bed material is less than the critical velocity (u_{cr}) and then there is no moving in sediment particles with flowing fluid. For condition stream velocity (u) exceeds (u_{cr}) the particles of sediments suspended in the flow and the scour generally referred to as live-bed scour.

Scour is classified in to three types:

- 1- Local scour
- 2- Constriction scour
- 3- General scour

Local scour is removal of sediments around structures due to fluid flow that cause disturbances in flow. Examples of the most common structures that cause local scour:

Bridge piers, underwater pipelines, sluice gates, spillways, etc. constriction scour it happen when there is a narrowing in the channel cause increasing in the velocity of flow .located in bridge alignments and causeway .general scour it happens without effects of any objects change the flow of fluid in the river. This study or research deals with local scour in live- bed condition resulting from the interaction of sample bridge pier with water flowing with different discharge. The removal of sediments around bridge pier affects on bridge safety and the foundation of pillar in view of this affects many life will loss under this condition. Bridge pier scour is a threat to the health of bridges and directly influences public safety. Studies in the United States report scour to be the second largest cause of failure among bridges, accounting for 15.5% of all failures (Ward hanaand Hadipriono, 2003).

1.2 Local scour

When there is an obstruction in flow pattern the flow will accelerate around the obstruction (like pier) also, in upstream of the pier an adverse pressure was formed, because this effects the upstream layer undergoes three dimensional separation at the end formed a horseshoe vortex these changes leads to increasing shear stress at the bed and if its greater enough lead to make a hole around the pier known as scour hole. Local scour can be form around any obstruction like bridges pile or bridge

abutments. There are two classifications of local scour, clear-water scour and live-bed scour, clear-water occurs when there are no movements of bed particles, the approach velocity in this case is less than critical velocity to move a particles and the shear stress of the bed is less than the critical shear stress to that make sediment movement in this case the growing of the scour hole will be suddenly and slowly going to equilibrium condition. The equilibrium condition can define as the points which scour depth will not be change means that the amount of sediments particles interrering the scour hole equal to the sediments particles removed from it by fluid flowing. Live-bed scour occurs when there is movement in bed particles the approach velocity in this case larger than critical velocity so it will be moving to bed particles, and the shear stress in the bed was larger than critical shear value. In order to all this the clear-water scour takes more time to reach maximum scour depth than live-bed scour, it is generally recognize that maximum of local clear-water pier scour is about 10 percent greater than the equilibrium of local live-bed pier scour (FHWA 1995), the Figure 1.1 illustrates that process.

1.3 Mechanism of Local scour

We can define a local scour that it is a moving of bed material around bridge pier located in moving water it is caused by three dimensional turbulent flow near bridge pier or any structure in moving water by increasing in water flow that resulting vortices and the vortex is a spinning, often turbulent, flow of fluid. Any spiral motion with closed streamlines is vortex flow. The motion of the fluid swirling rapidly around a center is called a vortex (vortex-Wikipedia) by an obstruction in river bed or any structure the vortices happened around that obstruction like bridge pier or abutment. “Since the velocity is decreasing from the surface to the bed, the pressure on the face of the pier also decreases accordingly forming a downward pressure

gradient. The pressure gradient hence forces the flow down the face of the pier, resembling that of a vertical jet. The resulting down flow impinges on the streambed and creates a hole in the vicinity of the pier base; the down flow impinging on the bed is the main scouring agent” (Melville and Raudkivi 1977). Figure 1.2 shows the flow and scour pattern at a circular pier under the action of currents.

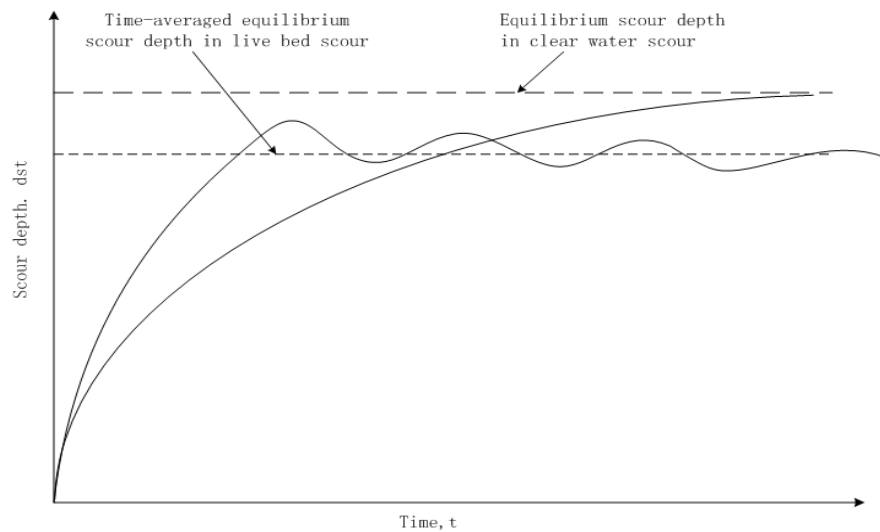


Figure 1.1 Time-dependent development of scour depth (Raudkivi and Ettema 1983).

In this research, study of scour depth depend on the time, the work was in hydraulic Laboratory of Gaziantep University Turkey with 8.3m length of flume 8.0m width and 9.0m depth with glass side and iron bottom to study the change in scour depth. Three Samples were used with 5 cm, 7.5 cm, and 11.1 cm diameter of pier sample that made from (PVC), different discharge taken in the test to see how the effects of discharge in equilibrium scour depth.

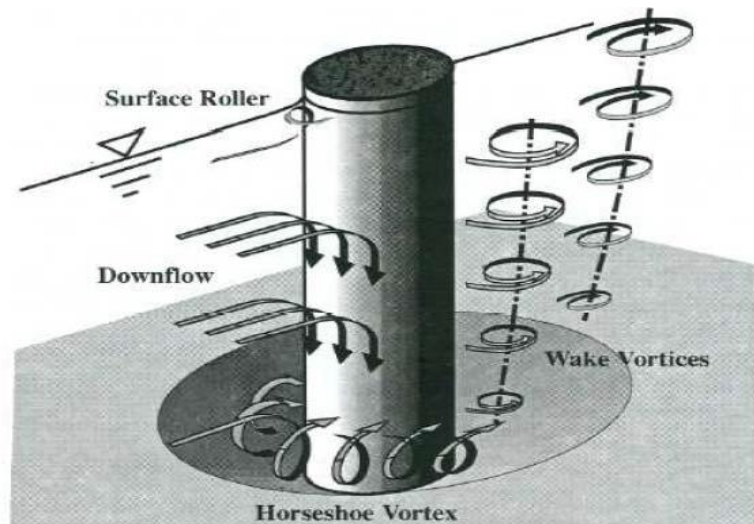


Figure 1.2 Flow and scour pattern at a circular pier (Melville and Coleman, 2000)

1.4 Objective of study

The objective of this study is to provide a means for predicting the temporal variation of live bed local scour around circular pier. The laboratory experiments was conducted with fixed bed material with 0.4mm mean size of the bed material, and with three different sample of bridge pier, and to predicting empirical equation to investigation equilibrium scour depth according to experimental results.

1.5 Layout of Thesis

The contents of each chapter can be explained as follows:

Chapter 1 Introduction: Introducing a brief history of scour around cylindrical bridge pier as well as explaining the principal objectives and layout of the thesis.

Chapter 2 Literature Review: This chapter covered previous work that deals with, local scour around cylindrical bridge pier, predicted maximum scour depth, parameter effecting on local scour.

Chapter 3 Experimental Work and Methodology: This chapter gives a description of the experimental apparatus, models and procedures.

Chapter 4 Results and Discussion: This chapter gives results and discussions of the results, analysis regression of the data obtain from experiments.

Chapter 5 Conclusion: the principal conclusions drawn from the results of the study and recommendations for future studies are presented in this study.

CHAPTER 2

LITERATURE REVIEW

2.1 Introduction

Many researchers worked on a local scour at bridge pier in alluvial bed to investigate an equation of predicting equilibrium maximum scour depth. This chapter attempts to summarize the present state of understanding of local scour at single bridge pier in sandy bed. Most of the research results that are available to predicting the maximum scour depth have been developed from small scale hydraulic modeling conducted in laboratories, and this section will cover available papers which discuss the predicting of temporal evolution of local scour.

2.2 Physical modeling of local scour around bridge pier

Experimental techniques and modeling in scour study is the best way to understand how the scour around bridge pier or abutment happened. Laboratory studies are needed to be more adequate in work and give us data that we need to compare with numerical data and develop it by an equation to predict a worse case. There are many researchers which are depending on laboratory data, to describe behavioral patterns around bridge pier scours. Some of them summarized the important work on local scour around bridge piers like Dargahi (1982) and Breusers et al. (1977). Hosny (1995) studied the effect of cohesive soils on local scour around cylindrical pier by using remolded clays in his experiments and found that the equilibrium scour depth in non-cohesive soils greater than in cohesive soils. He prepared an equation

to estimate maximum scour depth in cohesive soil in terms of the flow Froude number, compaction, initial water content and cylinder diameter.

Laursen (1963) studied the relationship of clear water scour in a long contraction as a function of geometry, flow, and sediment. He make model to study clear water scour he assume that clear water scour occurred when the boundary shear stress as a function of time is equal to critical attractive force and then he investigate an equation to estimate equilibrium scour depth for a bridge pile or abutment. Breusers H. N. C. (1977) make his experiments using pile width $d=5$ and 11 cm, and used sand with size $d_{50}=2$ mm.

Dey et al. (1995) carry out clear water scour experiments using two sand diameter, three approaching flow depth, three pier diameter, and six approach flow velocities, by depending on this experiments data he derived quasi-analytical equation for the flow filed by satisfying the continuity equation and determining empirical coefficients.

Yanmaz et al. (1991) was carried out in clear water scour case he used square and circular shape of piles, for circular shape the diameter was, 5.7 cm, 6.7 cm and 4.7 cm, using sand with size $d_{50}= 0.84$ mm and 1.07 mm.

Shen et al. (1966, 1969) developed an empirical equation for scour depth as a function of time and include pile diameter (d), and velocity (u), and depth of water (y), for developing empirical equation he depend on 21 experiments by using single cylinder diameter and size of sediments but with changeable in water depth to include live-bed scour and clear water scour around cylindrical pier with six-inch diameter, he used an adhesive material to fixed the sand bed and measured scour depth. Gosselin (1997)make series of experiments in clear water scour case he used a

pier (circular cylinder) with a diameter 17 cm, average flow velocity about $0.25 \text{ m}^2/\text{s}$, with median sand size about 0.17 mm, depth of flow 35 cm. He choose interval 1, 6, and 24 hour for stopped the flow and measured the depth and he calculated the velocities by Acoustic Doppler Aelocimeter (ADV).

Graf et al. (2001) studied on cylindrical bridge pier sample to investigate the flow patterns in plan of upstream and downstream by using Acoustic-Doppler Velocity Profiler (ADVP). They found that the turbulent kinetic energy was very great at the foot of the cylindrical bridge pier on the upstream side but compared to the approach flow the shear stress was reduced in the scour hole.

Mia, M and Nago (2003) study by experimental work to predict the local scour depth with time. He used a cylindrical pier under clear-water flows placed in uniform beds. By depends on sediment transport equation the pier scour depth was calculated. When the bed-shear stress tends to critical bed-shear stress the local scour depth reached to the Equilibrium. Therefore, at the circular bridge pier the changes to bed-shear stress should be included in the sediment transport theory.

Ming Zhao Liang Cheng (2010) studied local scours around a submerged vertical circular cylinder experimentally in steady currents and numerically. The experiments were conducted for two diameters of cylindrical pier the experiments conducted in water channel 4m wide, 45 m long, 2.5 m deep, the flume supply with pump $1 \text{ m}^3/\text{s}$ capacity. The section of the test was 4 m long, 4 m wide 0.25 m deep median size of the sand was $d_{50}=0.4 \text{ mm}$. Transient scour depth at the stagnation point (upstream edge) of the cylinder was measured using the so-called conductivity scour probes. Seabed topography around each cylinder pier was measured by using laser profiler. The effect of the height-to-diameter ratio on the scour depth was investigated in this

study. The experimental results show that the scour depth at the stagnation point is independent on cylinder height-to-diameter ratio when the later is smaller than two. The increase rate of equilibrium scour depth with cylinder height increases with an increase in Shields parameter.

Jau-Yau Lu and other (2011) works on cylindrical piers with unexposed foundation to estimate the temporal development of scour depth. A cylindrical pier with a foundation is considered as nonuniform pier. The concept of primary vortex and the principle of volumetric rate of sediment transport are used to develop a methodology to characterize the rate of evolution of the scour hole at nonuniform cylindrical piers. The scouring process includes three zones; Zone one having the scouring phenomenon similar to that of a uniform pier, Zone two in which the scour depth remains unchanged with its value equal to the depth of the top level of foundation below the initial bed level while the dimensions of the scour hole increase, and in Zone 3 the geometry pier foundation influences the scouring process. A concept of superposition using an effective pier diameter is proposed to simulate the scouring process in Zone 3. In addition, the laboratory experiments were conducted to utilize the laboratory results were used uniform sand with $d_{50} = 0.52$ mm having geometrical standard deviation of less than 1.4 The laboratory experiments were carried out in a 17 m long rectangular flume having a cross section of 0.6 m wide and 0.6 m deep at the Department of Civil Engineering, National Chung Hsing University, Taichung, Taiwan. The pier models made of plexiglass were embedded vertically in the middle of the sand recess of 7.5 m long, 0.6 m wide, and 0.25 m. The simulated results obtained from the proposed model are in good agreement with the present experimental results and also other experimental data. Also, the effect of unsteadiness of flow is incorporated in the model and the results of the model are

compared with the experimental data. The model agrees satisfactorily with the experimental data.

2.3 Scour prediction equation

There are more than 35 equations have been written for estimating the local scour at bridge pier according to McIntosh (1989). Most of local scour equations are based on research in laboratory flumes with noncohesive, uniform bed material and limited verification of results with field data (McIntosh, 1989). The equations are classified according to a local scour type if its live-bed scour or clear water scour and there are many methods to develop local scour equations by curveting or another method. Some of these equations are developed using regression method to compute maximum scour depths and the computing these results from predicted equations may be useful for design purposes because the results from these equations may give the designer more predict for risks and then to put a suitable factor of safety against local scour

1-Breusers equation

Breusers (1965) developed an equation for local scour depth at piers for tidal flow. Breusers concluded, that maximum depth of the scour was 1.4 times the pier diameter.

$$d_s = 1.4b \quad (2.1)$$

Where, b= pier diameter (m)

2-Laursen equation

Laursen and Toch (1956) developed equations by depend on experimental work in Iowa institute of hydraulic research, laursen and Toch equations assumes that flow depth is the most important factor in determining scour depth, but Shen (1966)

developed an equation assumed that velocity is important by including Froude number. The below equations (Laursen and Toch) are for square-nosed piers (Dr Les Hamill, (1999) Bridge hydraulic).

Live bed-scour:

$$d_{sp} = 1.5 b_p^{0.7} Y^{0.3} \quad (2.2)$$

Clear-water scour:

$$d_{sp} = 1.35 b_p^{0.7} Y^{0.3} \quad (2.3)$$

Where, d_{sp} is the pier scour depth (m), b_p is width of the pier (m), Y is the depth of approach flow (m).

Shen II equation;

$$d_{sp} = 3.4 b_p^{0.67} F^{0.67} Y^{0.33} \quad (2.4)$$

where F is the Froude number of the approach flow.

3-Larras equation

Larras (1963) he depends on field investigation to get the required data in several French rivers and scale-model investigation to developed Larras equation:

$$y_s = 1.42 K_{S2} b^{0.75} \quad (2.5)$$

Where K_{S2} is a coefficient based on the shape of the pier nose (1.0 for cylindrical piers and 1.4 for rectangular piers). Where y_s and b in ft.

Larras measured scour depth after a flood had passed, there for the equation depends on pier width and shape only (Shen and others, 1969).

4-Hydraulic engineering circular 18 (HEC-18) equations

The Federal Highway Administration report “Hydraulic engineering circular 18 (HEC-18): Evaluating scour at bridges” (Richardson and others, 1993) presents the following equation that was developed using laboratory data for circular piers scour

$$\frac{y_s}{y_o} = 2 K_1 K_2 K_3 \left(\frac{b}{y_o} \right)^{0.65} F_o^{0.43} \quad (2.6)$$

where K_1 is a coefficient based on the shape of the pier nose ($K_1=1.1$ for square-nosed piers, 1.0 for circular nosed piers, and 0.9 for sharp nosed piers);

K_2 is a coefficient based on the ratio of pier length to pier width (L/ b) and the alignment of the approach flow to the bridge pier, (Table 2.1) below show coefficient for pier alignment (Richardson et al, 1993).

Table 2.1 Coefficient for pier alignment (K_2) for the HEC-18 Equations (Richardson et al, 1993)

Angle	L/b=4	L/b=8	L/b=12
0°	1	1	1
15°	1.5	2	2.5
30°	2	2.75	3.5
45°	2.3	3.3	4.3
90°	2.5	3.9	5

Table 2.2. Bed-condition correction factor (K_3) for the HEC-18 Equation (Richardson et al, 1993)

Bed condition	Dune height	* K_3
Clear-water scour	N/A	1.1
Plane bed and antidune flow	N/A	1.1
Small dunes	0.6 to 3.0 m	1.1
Medium dunes	3.0 to 9.0 m	1.1 to 1.2
Large dunes	> 9.1 m	1.3

* K_3 is a coefficient based on channel bed conditions.

5-Melville and Sutherland (1988)

Melville and Sutherland developed equation based on laboratory experimental was conducted in New Zealand, this equation called Melville and Sutherland equation

$$d_s = K_1 K_d K_y K_\alpha K_s b \quad (2.7)$$

Where k_1 is a coefficient for flow intensity, k_d is a coefficient for sediment size, k_y is a coefficient for flow depth, k_α is a coefficient for flow alignment k_s is a coefficient for pier shape

Table 2.3. Summary of predicted equilibrium scour depth equations

Researcher	Equations	Description
Breusers (1965)	$d_s = 1.4b$	d_s is maximum scour depth b is pier diameter
Laursen and Toch (1956)	$d_{sp} = 1.5 b_p^{0.7} Y^{0.3}$	d_{sp} is the pier scour depth (m), b_p is width of the pier (m), Y is the depth of approach flow, for live bed scour
Laursen and Toch (1956)	$d_{sp} = 1.35 b_p^{0.7} Y^{0.3}$	For clear-water scour
Shen II	$d_{sp} = 3.4 b_p^{0.67} F^{0.67} Y^{0.33}$	F is the Froude number of the approach flow
Larras (1963)	$y_s = 1.42 K_{S2} b^{0.75}$	K_{S2} is a coefficient based on the shape of the pier nose
HEC-18 equation	$\frac{y_s}{y_o} = 2 K_1 K_2 K_3 \left(\frac{b}{y_o}\right)^{0.65} F_o^{0.43}$	F is a Froude number $K_1 K_2 K_3$ is coefficient
Melville and Sutherland (1988)	$d_s = K_1 K_d K_y K_\alpha K_s b$	
Raudkivi and Ettema(1983)	$y = 2.3bK\sigma$	where $K = f(\sigma_g) = 1$ for uniform sediment, $\sigma_g =$ geometric standard deviation of the grain size distribution
Shen et al. (1969)	$y_{se} = 0.000223R_b^{0.619}$	where $R_b =$ pier Reynolds number

2.4 Parameter affecting on local scour

2.4.1 Pier geometry

Pier width is an important effect on pier geometry also on scour of pier, piers that have a uniform width and shape with elevation are uniform piers, while if it vary in shape or width with elevation are nonuniform piers. Most researches used a uniform

pier with cylindrical shape, in the field, bridge piers have different shapes and sizes cylindrical piers with round or square noses are more commonly used. Many previous equation to estimate scour depth include pier width as an depending variable, the equation that did not include pier width it based on experiments using piers with fixed shape, (Melville and Sutherland 1988) suggested that the maximum depth of scour is 2.4 times the pier width. (Richardson and others, 1993) recommends 2.4 times the pier width as a limiting depth of scour for flows aligned with round-nosed piers. The many researchers studied the effected of pier nose shape on the depth of scour, table 2-4 shows the coefficients for correcting the scour depth for pier shape. Laursen and Toch (1956) coefficient for pier shape is widely used in the pier scour prediction equation.

2.4.2 Sediment coarseness and gradation

Melville and Coleman (2000) defined the sediment coarseness and the ratio of the pier width (D) to the mean grain size of the sediment (d_{50}). According to the Melville and Coleman the local scour is affected by the sediment size when the ratio of pier width (D) to the mean sediment size (d_{50}) less than 50, ($D/d_{50} < 50$). When the $D/d_{50} > 50$ the local scour is not affected by the sediment coarseness. Another property of sediments it is geometric standard deviation of sand size, $\sigma_g \left(\frac{d_{84}}{d_{16}}\right)^{1/2} \cdot \sigma_g$, It's about 1.8 for natural river sand while for uniform sand σ_g is about 1.3 (Hoffmans and Verhejj 1997). There are many studies about the effect of sediment gradation on local scour depth one of these study is Ettema (1980). He studied on circular pier under clear-water scour condition, conducted his experiments at the threshold of motion condition for the median size of the sediment material used. The experiments shows that the rate of scour hole development and the equilibrium scour depth

Table 2.4 Coefficient of pier shape

Shape	Length- width ratio	Tison (1940)	Laursen&toe h (1956)	Chapert&En geldinger (1956)	Garde (1961)	Venkatadri (1965)	Neill (1973)	Dietz (1972)
Circular	1	1.0	1.0	1.0	1.0	1.0	1.0	1.0
Lenticular	2		0.91		0.9			
	3		0.76		0.8			
	4	0.67		0.73	0.7			
	7	0.41					0.8	
Triangular Nose 60°					0.75		0.65	
Triangular Nose 90°					1.25		0.76	
Rectangular	1							1.22
	2		1.11					
	3							1.08
	4	1.4		11.1				
	5							
	6			1.11				0.99
Rectangular chamfered								1.01

decrease as the standard deviation of the particle size distribution increases, and armoring occurs. For nonuniform sediment material (i.e. at a higher value of σ_g) on the approach flow bed and at the scour hole base around the threshold condition, $u^*/u_{*c} \approx 1$. The armoring leads to a large decrease of the local scour depth. However, sediment nonuniformity has only a small effect on the scour depth at a high value of u^*/u_{*c} , where the flow is capable of entraining most grain sizes within the non-uniform sediment.

2.4.3 Temporal development of scour

The local scour in the surrounding area of bridge pier depending on time. Time development of scour is the stage of maximum scour depth reached in given time. The most of the literature that given (about flow, pier shape and sediment condition) is on determination of the maximum equilibrium scour depth. The time development of scour takes large area in most researchers' research (e.g. Melville and Chiew 1999; Mashair et al 2004). Dey (1999) was also seen that time is an important factor in studies of scour. The temporal development of scour is depending on condition of flow, pier geometry and sediment parameters (Melville and Chiew 1999).

Melville and Chiew (1999) studied the temporal development of scour at bridge pier under clear-water flow conditions and developed equations for estimating the local depth. In an attempt to consolidation the criteria for reaching an equilibrium state, Chiew and Melville (1999) collected data from about (35) experiments that covered a large range of pier diameter, flow depth, and approach flow velocities. Two different sediment diameters in the coarse range were in use. The tests were allowed to run until equilibrium was reached. The author shows that the time of equilibrium is the time when the rate of scour was reduced to 5 percent (5%) of the pier diameter in a 24 hour period. This standard yielded values of time to equilibrium as high as 3 days

for some cases. The data indicated that the time of equilibrium increases with increasing pier diameter for a given approach flow depth and velocity ratio. The data also showed that, the time to equilibrium scour condition increases with an increase in the velocity ratio. For bridge piers under clear-water conditions, the equilibrium time scale increases rapidly with flow intensity, reaching a maximum at the threshold condition (Melville and Coleman 2000; Melville and Chiew 1999). The authors noticed that there is correlation between the time required to reach equilibrium scour and the equilibrium of scour depth. Melville and Chiew (1999) concluded that both the depth of scour at equilibrium and the time required to reach equilibrium scour are influenced similarly by the same set of sediment parameters and flow. As shown in Figure 2.1, Ettema (1980) noted that, when the depth of scour was plotted versus the logarithm of time, there were three different phases of the scour process. He referred to the three phases as the initial phase (1), the erosion phase (2), and the equilibrium phase (3). As shown in the Figure 2-1, in the initial phase (i.e., region 1), rapid scouring occurs due to the down flow at the pier face impinging on the planar bed. This phase is characterized by a steep on the diagram. The second phase, which is known as the primary eroding phase, starts when the horseshoe vortex starts to dominate the scouring process. The main erosion occurs at the front of the pier. During the erosion phase (i.e., region 2 in Figure 2.1), the scour hole increase as the horseshoe vortex grows in both size and strength. The slope of the line in this phase is much less than in the previous phase. In the third stage (final), called the equilibrium phase (i.e., region 3 in Figure 2.1), the equilibrium depth has been attained and therefore no further scour occurs as the horseshoe vortex ceases to excavate further. At this point, the slope of the line is zero.

2.4.4 Flow intensity

The intensity of flow is defined as the ratio of the shear velocity (u^*) to the critical shear velocity (u^*_c) or it is ratio of the approach mean velocity to the critical mean velocity (Melville and Chiew 1999). Under clear-water conditions, the local scour depth in uniformly-graded sediment increases almost linearly with velocity to a maximum at the threshold velocity (Melville and Coleman, 2000). When the ratio $u^*/u^*_c = 1$, scour depth reached to the maximum and the corresponding maximum

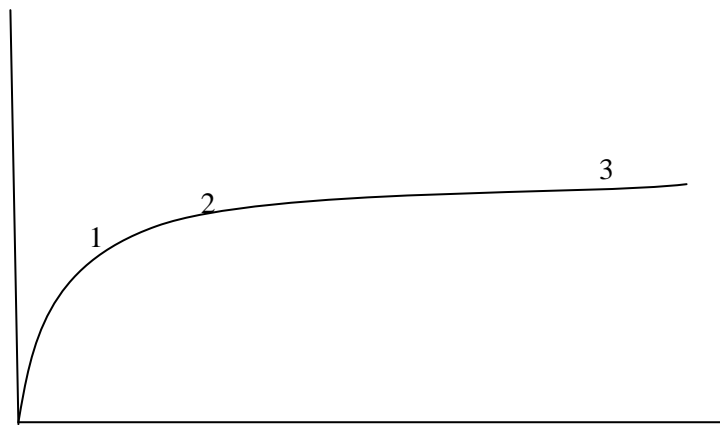


Figure 2.1 Schematic diagram of the three different phases of the scour process
(Modified from Ettema 1982)

scour depth is called the threshold peak. As the velocity exceeds the threshold velocity, the local scour depth in uniform sediment first decreases and then increases again to a second peak, but the threshold peak is not exceeded. Because of sediment is uniform. The same direction was observed by Chabert and Engeldinger (1956), Raudkivi and Ettema (1983), Ettema (1980), Breusers et al. (1977), Chiew (1984), Laursen and Toch (1956), and. The general conclusion was that maximum scour depth in uniform sediments happen at the threshold condition for the clear-water local scour situation.

2.4.5 Pier size

Experiments have clearly shown that it is possible to relate the scour depth to the size of the pier (Breusers et al. 1977). This observation can be explained physically by the fact that scouring is due to the horseshoe vortex system whose dimension is a function of the diameter of the pier. It has also observed by Shen et al. (1969) that the horseshoe vortex, being one of the major scouring agents, is proportional to the pier Reynolds number (R_b), ($R = uD/ \nu b$), which in turn is a function of the pier diameter. For the same value of mean approach flow velocity, hence, the depth of scour is proportional to the pier width. The influence of pier size on the local scour depth is of interest when data from the laboratory are interpreted for field use (Breusers and Raudkivi 1991). Under clear-water situation, pier size influences the time taken to reach the ultimate scour depth but not its relative magnitude y_s/D , if the influence of relative depth, y_o/D , and relative grain size D/d_{50} on the local scour depth are excluded (Breusers and Raudkivi 1991). They also concluded that the volume of the local scour hole formed around the upstream half of the perimeter of the pier is proportional to the cube of the pier diameter (or the projected width of the pier). The larger pier, the larger scour hole volume and also the longer is the time taken for the development of the scour hole for a given shear stress ratio.

2.4.6 Flow depth

The effect of flow depth on the scour depth has been studied by many researchers (e.g. Melville and Coleman 2000; Hoffmans and Verheij 1997; Breusers and Raudkivi 1991; Ettema 1980; Dey 1977; Breusers et al. 1977; Chabert and Engeldinger 1956; Laursen and Toch, 1956). Because presence of the pier in the channel the surface roller around the pier and a horseshoe vortex at the base of the pier will happen, The local scour depth affected by Flow depth when the horseshoe

vortex is affected by the formation of the surface roller that forms at the leading edge of the pier the two rollers, the bow wave and the horseshoe vortex, rotate in opposite directions. In principle, the local scour depth does not depend on the flow depth but depends only on the diameter of pier, as long as; there is no interference between the bow wave and the horseshoe vortex. In case flow depth decreases, the roller of surface becomes relatively more prevailing and causes the horseshoe vortex to be less able of entraining sediment, so, for the flow at shallow depth the local scour depth is reduced.

There is classification for the influence of the flow depth in relation to the width of the pier (Melville and Coleman 2000), for shallow flow, D/y_o , (where D is pier diameter and y_o is flow depth) Table 2.5, as adapted from Melville and Coleman, shows a classification of local scour processes at bridge pier foundations.

Table 2.5 Classification of local scour depending on D and y_o at bridge pier foundations

Class	D/y_o	Local scour dependence
Narrow	$D/y_o < 0.7$	$y_s \propto D$
Intermediate width	$0.7 < D/y_o < 5$	$y_s \propto (D y_o)^{0.5}$
Wide	$D/y_o > 5$	$y_s \propto y_o$

In summary, observations showed that at shallow flow depths the local scour at piers increases with flow depth, but for deep flow the scour depth becomes independent of flow depth but depends on the pier diameter.

CHAPTER 3

EXPERIMENTAL STUDY AND METHODOLOGY

3.1 Introduction

In this chapter, the experimental studies were conducted in the hydraulic laboratory at University of Gaziantep Turkey. The experimental study reported in this thesis pertains to the measurement of the scouring development around circular bridge piers. The experimental set-up is described in this chapter.

3.2 Experimental flume

Experiments in this study were conducted in a circulating flume as shown in Figure 3.1 Length of the flume is about 8.3 m, width is 0.8 m, and depth is 0.9 m with glass sides and iron bottom. The study section was about 2.8 m from inlet of the flume which is filled with sand, medium size of the particles $d_{50}= 4\text{mm}$. The thickness and width of the sand is 0.2m and 0.8m respectively, the length of the test section is about 1.5m. The circulating flow system is served by a pump with capacity of 25 lt/sec located at the right of the flume and there is a valve to control the flow in the flume as shown in figure 3.3. The pump withdraws the water from a sump at the downstream of the flume. At the end of the flume, there is a rectangular weir to measure the flow rate and there is a point gage sliding along the flume to measure the depth of the scour hole. In order to have uniform flow before and after the bridge pier, a ramp was constructed and fixed to the upstream and downstream of the test section of the flume. Experiments were carried out at fixed discharges. Figure 3.1 and 3.2 shows the flume and the model of bridge pier above the bed material.



Figure 3.1 General View of the Laboratory Flume



Figure 3.2 General View of the Bridge Pier

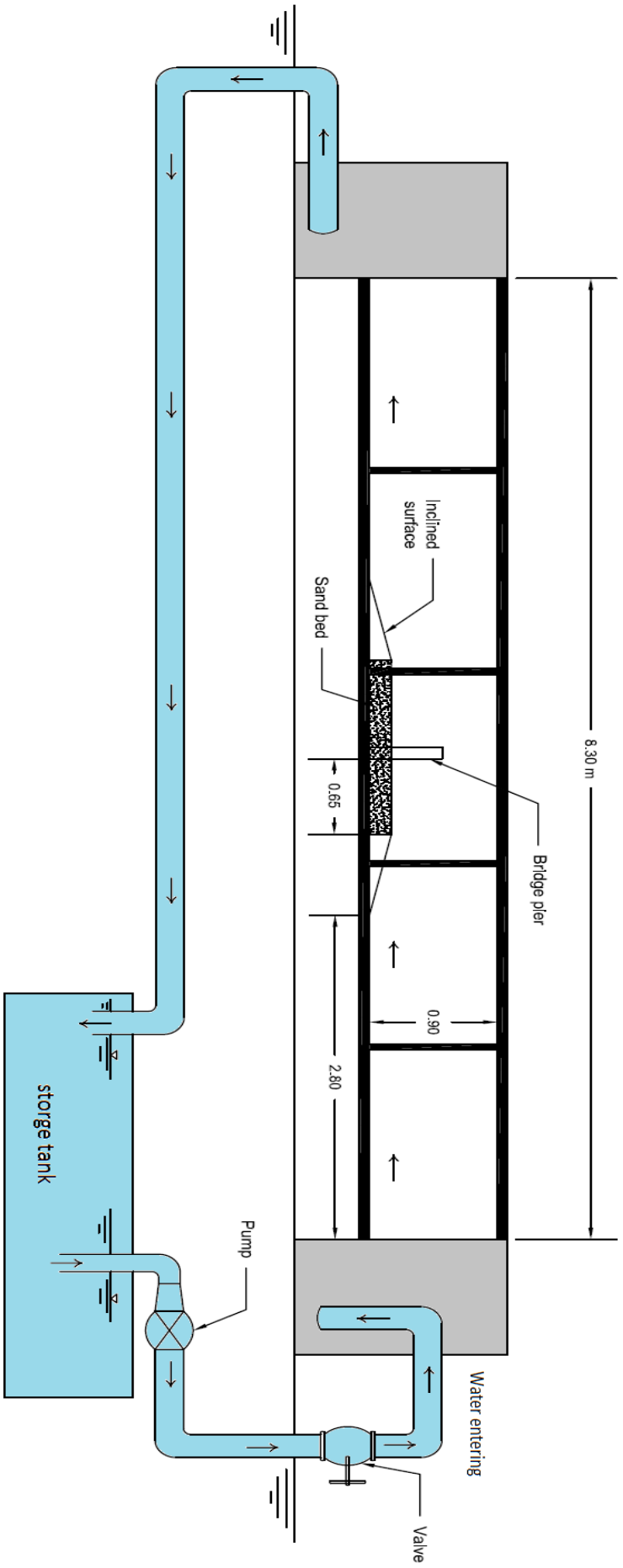


Figure 3.3 Schematic illustration of the experimental flume system

3.3 Bridge Pier Models

The models of the pier were made from Polyvinyl Chloride (PVC) pipe. Three circular shape of piers model with the diameter of 50 mm, 75 mm, and 110 mm were used in this study as shown in Figure 3.4. In each one, the pier was located on the centerline of the channel, it's important especially when measuring a contour profile of the scour hole, also to reduce the side effects of the flow around the cylindrical pier.

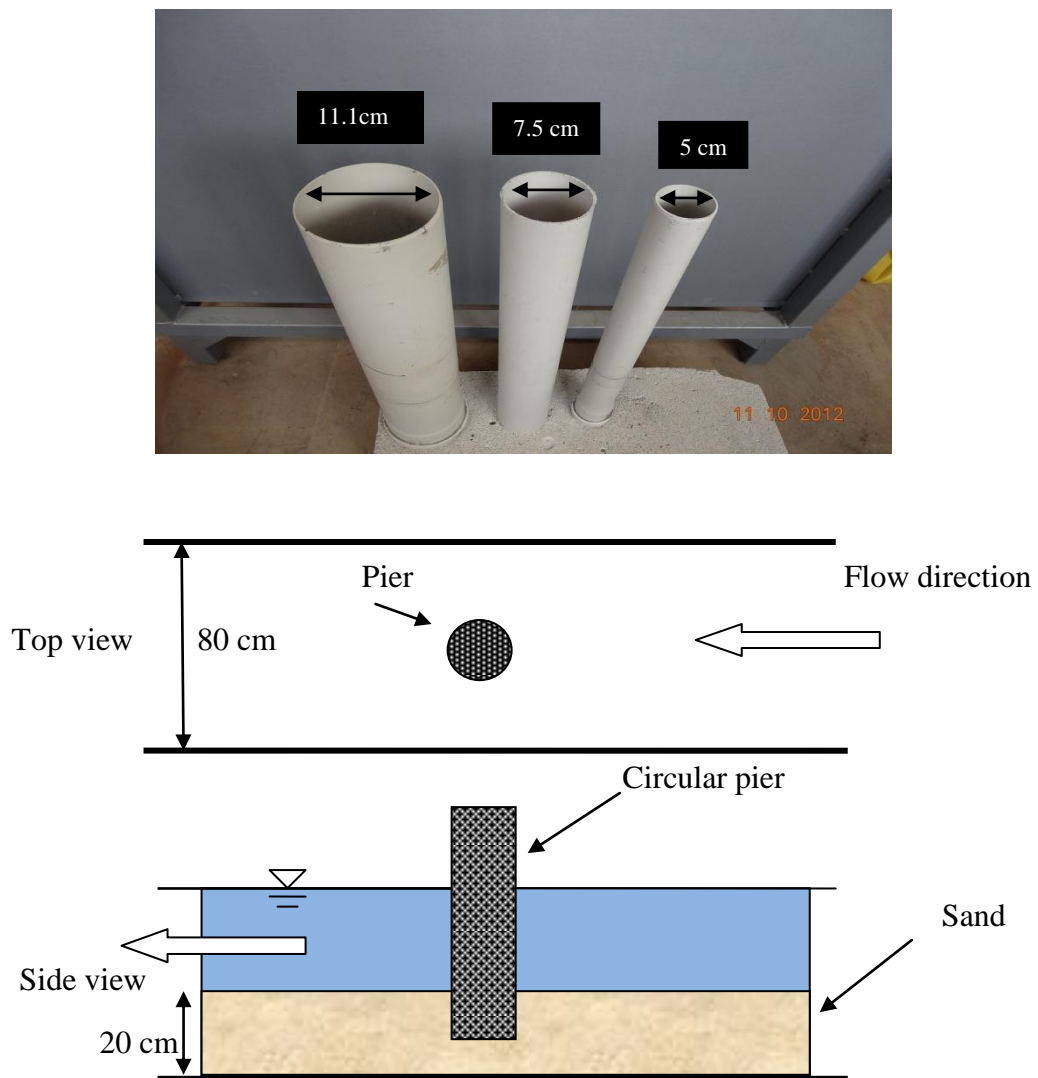


Figure 3.4 Pier model

3.4 Sand bed

A series of tests were carried out to characterize the sand bed material present in the flume used for the study. The soil tests were carried out of mechanical sieve analysis and a specific gravity test. The results of these tests showed that the bed material with a median particle size $d_{50} = 4$ mm and a specific gravity $G_s = 2.68$. The geometric standard deviation of the sand size, σ_g , is 1.15mm, which implies that the sand is of uniform size distribution. The σ_g is defined as, $\sigma_g = (d_{84}/d_{16})^{0.5}$. The plot of the grain size distribution (sieve analysis) test is depicted in Figure 3.5. The pier diameter was also carefully chosen so that there was negligible effect of sediment size on the depth of scour. (It is known that the bed material grain size does not affect the depth of scour if the pier width to grain size ratio exceeds a value of about 50) (Ettema 1980), in this study that ratio are about 12.5 and 18.75 and 27.5 for the pier diameter 50 mm, 75mm, 110 mm, respectively, that means the bed material effect on the local scour depth.



Figure 3.5 Sand specific gravity field test

In this study, different size of sediment was tested to determine the median particle size d_{50} . The sieve analyses of the sediment, which were used in the present experiments, are given in Figure 3.6.

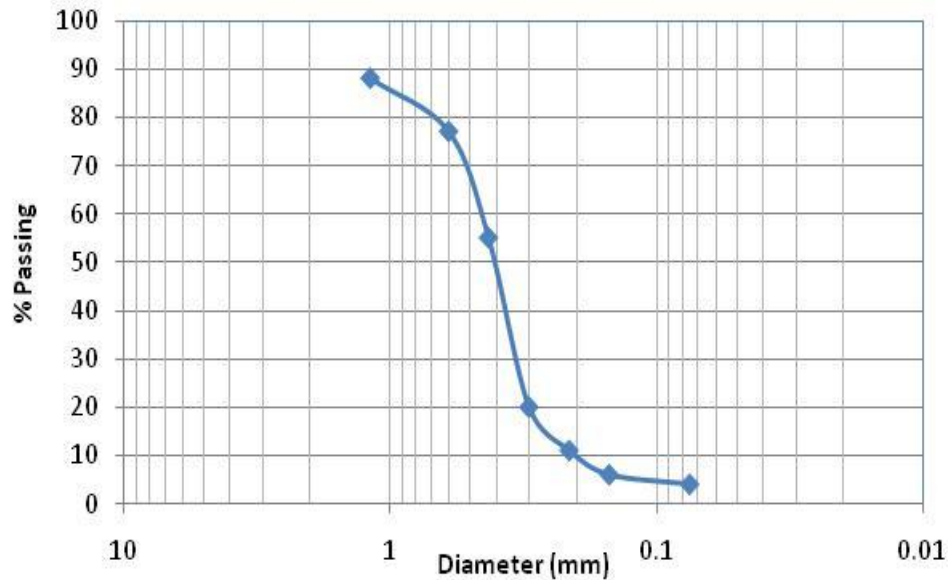


Figure 3.6 Grain size distribution (sieve analysis)

3.5 Experimental methodology

3.5.1 Program of the work

In this study, the temporal development was observed by taking three bridge pier models having diameters of 50 mm, 75 mm, and 110 mm respectively. Four discharges were used (6.29 lt/s, 16.081 t/s, 22.63 lt/s, and 25.19 lt/s). All the experiments with different pier diameter at different discharges are continued until the scour reaches to the equilibrium scour depth. Then the test will stop and record the time of equilibrium scour depth. Point gage was used to measure the scour hole profiles around bridge pier model, the variation of local scour depth with time is measured at various time by stopping the experiments and run it again. Rectangular weir was used to measure the discharge. Calibration of the rectangular weir was done using measuring test.

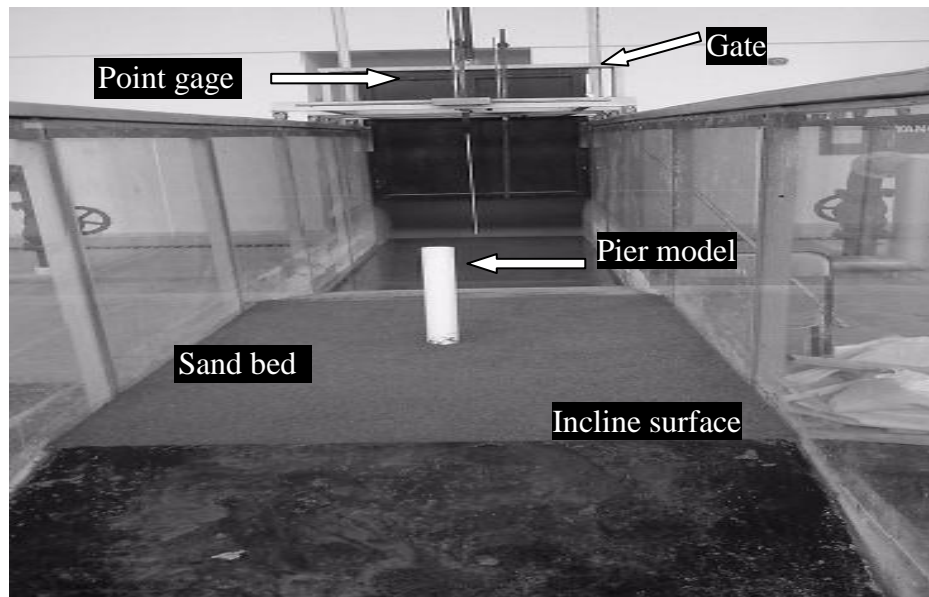


Figure 3.7 Experimental setup

3.5.2 Experimental procedure

Firstly, the pier model was first put in the flume at the half width and 0.65 m away from the begin of the test section in the flow direction, Before each run, care was taken to level the sand bed during the entire length of the flume and especially close to the pier using an Aluminum screed to give the sand bed a smooth and uniform surface, by using point gage, where supported by the mobile carriage of the flume, initial bed elevations were measured from in front of pier model to check the leveling of the sand bed before scour process. The system was run until the flume fill up with water, by using electronic stopwatch the time will recorded when water close to the bridge pier model, after completing each run the pump will stopped and then carefully measured scour hole depth without disturbing scour topography, and every 5 minutes scour depth was measured by point gage until reach to the equilibrium scour depth. After the scour depths reached to equilibrium depth, the pump will stopped and water was drained from test section to measure the maximum scour

depth and to take contour profile by using point gage were divided the test section by grid of 5 cm interval then using computer software called Surfer© version 10 (Surfer is a grid-based mapping program that interpolates irregularly spaced XYZ data into a regularly spaced grid. The grid is used to produce different types of maps including contour, vector, image, shaded relief, 3D surface, and 3D wireframe maps) to draw contour map. In this study, surfer convert topographical scour hole data in to counter maps and three-dimensional profile maps this point will be discussed in Chapter 4. As shown in Table 3.1 the test was divided in to three groups, group one includes pier diameter of 5 cm was tested with four discharge (6.29 lt/s, 16.08 lt/s, 22.63 lt/s, and 25.19 lt/s) respectively, then observed the scour depth for each discharge by compare it with other groups (different diameter), Group 2 includes pier diameter of 7.5 cm and Group 3 includes pier diameter of 11.1 cm it's also tested with four discharge as shown in Table 3.1. The maximum scour depth in group three greater than group two and one, more details will be discussed in Chapter 4.

Table 3.1 Experimental conditions

Run	Diameter (d) (cm)	Flow depth (h) (m)	Time (t) (min)	Discharge (Q) (l/s)	Velocity (u) m ² /sec	Froude Number (Fr)	Scour depth (d _{sc}) (cm)
			GROUP	ONE			
SA1	5	0.025	15	6.29	0.3145	0.635062	6
SA2	5	0.044	30	16.6	0.454545	0.691857	7.7
SA3	5	0.054	30	22.63	0.528636	0.726316	8.2
SA4	5	0.058	30	25.19	0.542888	0.719717	8.5
			GROUP	TWO			
SB1	7.5	0.025	50	6.29	0.3145	0.635062	6.1
SB2	7.5	0.044	50	16.6	0.454545	0.691857	9.1
SB3	7.5	0.054	50	22.63	0.528636	0.726316	9.7
SB4	7.5	0.058	60	25.19	0.542888	0.719717	10.5
			GROUP	THREE			
SC1	11.1	0.025	30	6.29	0.3145	0.635062	6.4
SC2	11.1	0.044	40	16.6	0.454545	0.691857	11.2
SC3	11.1	0.054	35	22.63	0.528636	0.726316	11.7
SC4	11.1	0.058	30	25.19	0.542888	0.719717	11.9

CHAPTER 4

RESULTS AND DISCUSSION

4-1 Introduction

In this chapter, the laboratory results for temporal development of local scour around bridge pier with different pier diameters were studied. A formula for predicting the maximum scour depth was found. Computer software called Surfer used to draw contour maps and three-dimensional profile maps. In this chapter, experimental results in terms of temporal development of scour will be compared with predicted maximum scour equations that described in the literature for other researchers.

4.2 Local scour depth

Maximum local scour depth was measured in 3 experimental groups of run, Group 1 tests were conducted with a 5 cm pier diameter with 4 discharges of 6.29 lt/s, 16.6 lt/s, 22.63 lt/s, and 25.19 lt/s, these experimental runs are shown in Table 3.1 as SA1, SA2, SA3, and SA4.

4.2.1 Measurement of local scour depth with $d=5$ cm and $Q=6.29$ lt/s

The effect of the scouring process was noticed immediately upon starting the test. Table 4.1 summarizes a test condition and showing temporal development of scour depth with discharge of 6.29 lt/s. Figure 4.1 shows development of local scour depth with respect to time. Scour depth reached to equilibrium in 20 minutes. The maximum scour depth was measured as 0.06 m and flow depth of 0.025 m. Figure 4.1 shows that scour depth increases in first 10 minutes.

Table 4.1 Temporal development of scour depth for SA1 ($d = 5\text{cm}$, $Q = 6.29\text{ lt/s}$)

Time (t) (min)	Discharge (Q) (lt/s)	max. scour (dse) (m)	Flow depth (y) (m)
1	6.29	0.033	0.025
2	6.29	0.043	0.025
3	6.29	0.047	0.025
4	6.29	0.05	0.025
5	6.29	0.052	0.025
10	6.29	0.058	0.025
15	6.29	0.06	0.025
20	6.29	0.06	0.025
25	6.29	0.06	0.025
30	6.29	0.06	0.025

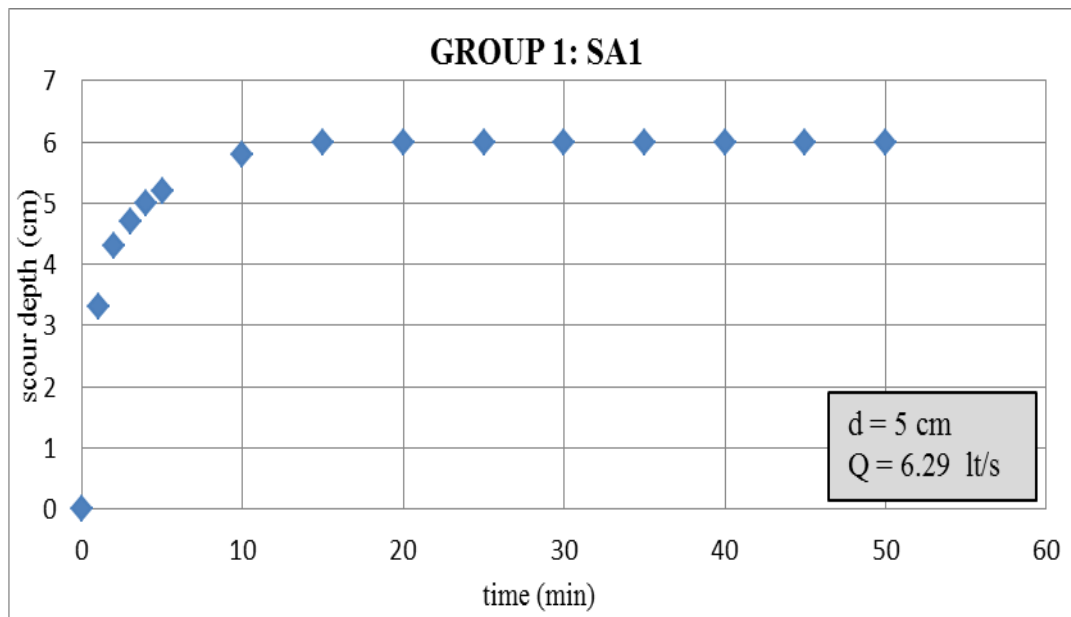


Figure 4.1. Time evolution in scour depth for $d= 5\text{cm}$, $Q=6.29\text{ lt/s}$

4.2.2 Measurement of local scour depth with $d=5\text{ cm}$ and $Q=16.6\text{ lt/s}$

In this test, the discharge was increased from 6.29 lt/s to 16.6 lt/s . Because of increases in discharge the flow depth increased to 0.044m . Table 4.2 shows, that the scour depth becomes 0.049 m after 1 minute and it becomes 0.077 m after 45 minutes. The experimental results shows that the maximum scour depth in SA2

greater than SA1, that means the maximum scour depth increases with increasing discharge.

Table 4.2. Temporal development of scour depth for SA2(d= 5cm, Q=16.6 lt/s)

t (min)	Q (lt/s)	d _{se} (m)	y (m)
1	16.6	0.049	0.044
2	16.6	0.055	0.044
3	16.6	0.056	0.044
4	16.6	0.057	0.044
5	16.6	0.058	0.044
10	16.6	0.065	0.044
15	16.6	0.068	0.044
20	16.6	0.07	0.044
25	16.6	0.072	0.044
30	16.6	0.074	0.044
35	16.6	0.077	0.044
40	16.6	0.077	0.044
45	16.6	0.077	0.044

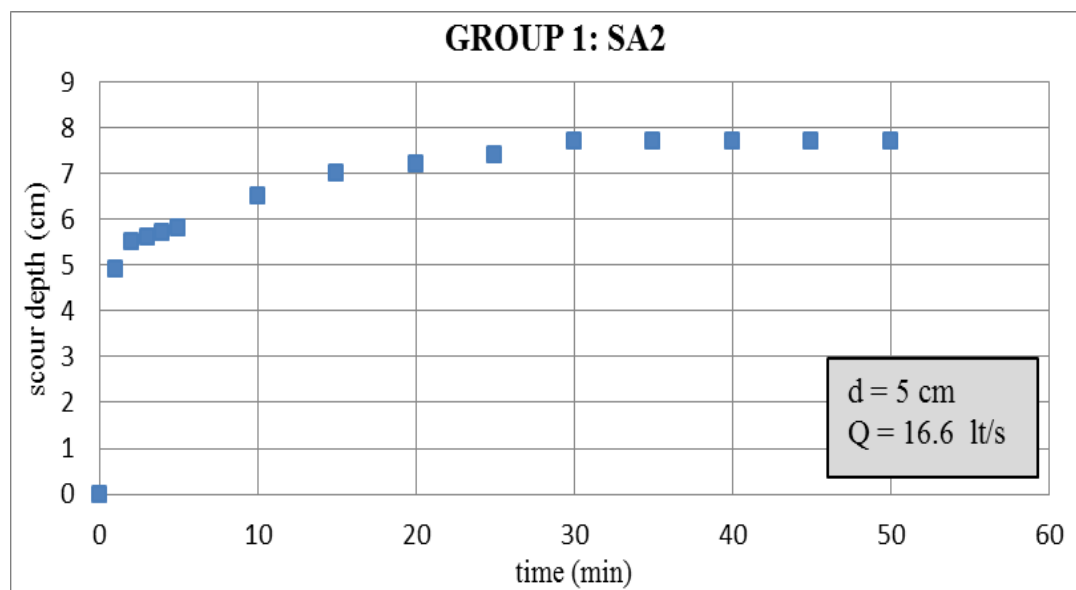


Figure 4.2. Time evolution in scour depth for d= 5cm, Q=16.6 lt/s

Figure 4.2 shows, time development of maximum scour depth for the 5 cm diameter of pier. Equilibrium scour depth increases when approaching discharge to the pier increases. The reason is that the kinetic energy of the flow increases and destructive effect of the flow increases. Many bridges are collapsed during the flood season. Because of this, the pier should be designed for maximum predicted discharge.

4.2.3 Measurement of local scour depth with $d=5$ cm and $Q=22.63$ lt/s

In this tests, the discharge increases from 16.6 to 22.63 lt/s. After 30 minutes the maximum scour depth becomes 0.082 m as shown in Table 4.3. The maximum scour depth increases with increasing approaching discharge to the bridge pier.

Table 4.3. Temporal development of scour depth for SA3($d= 5$ cm, $Q=22.63$ lt/s)

t (min)	Q (lt/s)	d_{se} (m)	y (m)
1	22.63	0.052	0.054
2	22.63	0.056	0.054
3	22.63	0.06	0.054
4	22.63	0.064	0.054
5	22.63	0.068	0.054
10	22.63	0.071	0.054
15	22.63	0.076	0.054
20	22.63	0.078	0.054
25	22.63	0.081	0.054
30	22.63	0.082	0.054
35	22.63	0.082	0.054
40	22.63	0.082	0.054

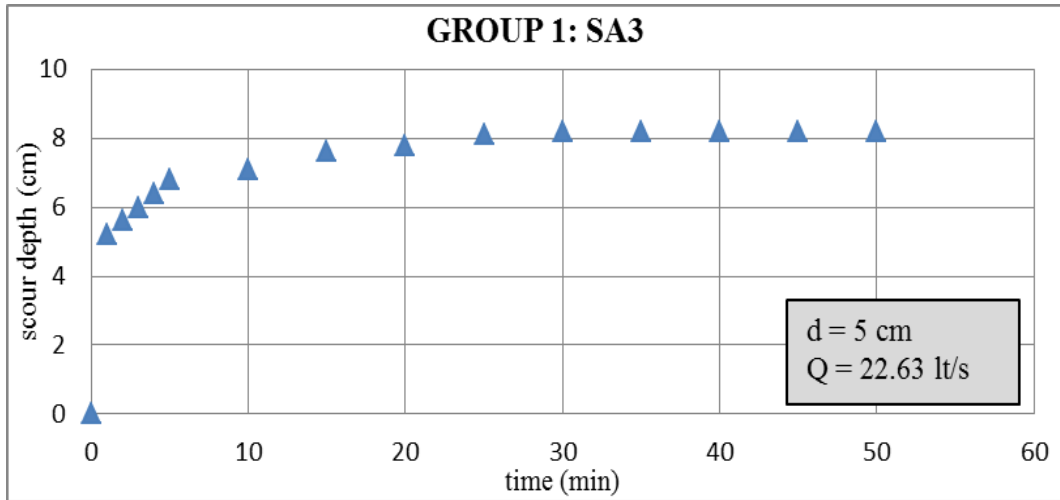


Figure 4.3. Time evolution in scour depth for $d= 5\text{cm}$, $Q=22.63\text{ lt/s}$

Figure 4.3 shows that the scour depth becomes 0.052m in 1 minutes. The maximum scour depth becomes 0.085 after 30 minutes. The present experimental results show that, scour depth increases much quicker when approaching discharge increases.

4.2.4 Measurement of local scour depth with $d=5\text{ cm}$ and $Q=25.19\text{ lt/s}$

The test of SA4 is the final test in Group 1. Maximum discharge of 25.19 lt/s was used in this test. Equilibrium scour depth occurred in 25 minutes with a flow depth of 0.058 m.

Table 4.4 Temporal development of scour depth for SA4 ($d = 5\text{ cm}$, $Q = 25.19\text{ lt/s}$)

t (min)	Q (lt/s)	d_{se} (m)	y (m)
1	25.19	0.048	0.058
2	25.19	0.054	0.058
3	25.19	0.058	0.058
4	25.19	0.062	0.058
5	25.19	0.065	0.058
10	25.19	0.073	0.058
15	25.19	0.78	0.058
20	25.19	0.08	0.058
25	25.19	0.085	0.058
30	25.19	0.085	0.058

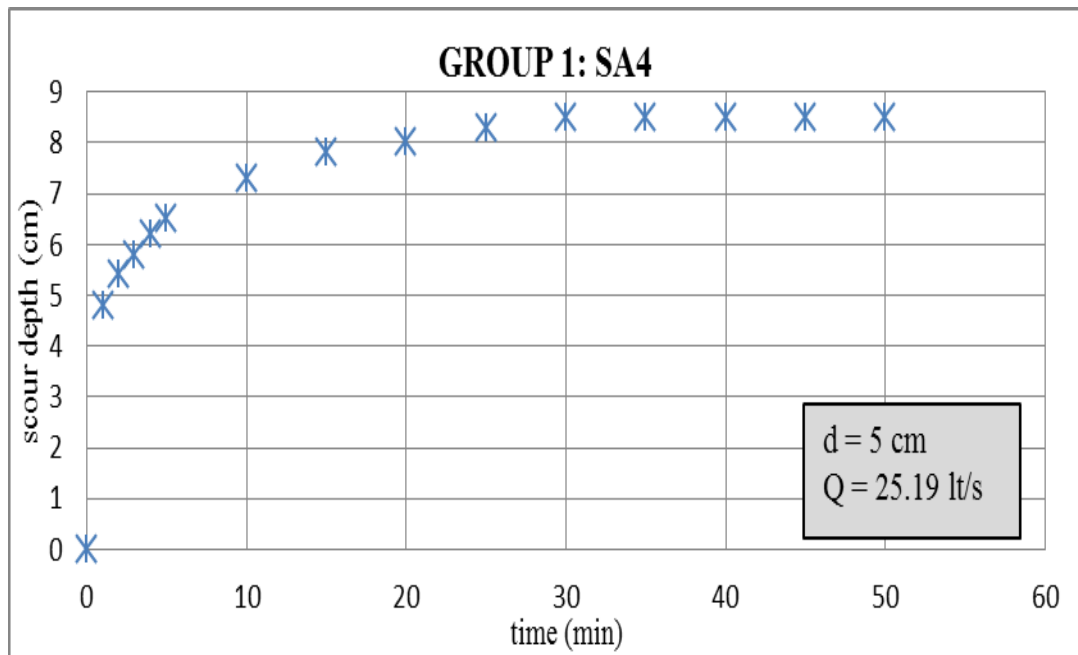


Figure 4.4 Time evolution in scour depth for $d=5\text{ cm}$, $Q=25.19\text{ lt/s}$

Figure 4.4 shows the development of scour depth with respect to time. The scour started first at sides of cylindrical pier sample and then rapidly scour hole moved from both sides to toward centerline of the pier at the upstream. During this time there was a ring like groove formed at nose of pier face (upstream face), after 5 minutes approximately from running the test, ripple was forming downstream as shown in Figure (4.11 a), behind the cylindrical pier at centerline, the deposition of sediment also occurs due to the transport of sediment from scour hole. Maximum scour point which located at the side of the bridge pier and by over time the maximum scour point moved to upstream of pier. By continue in scour process the sand material that going out from scour hole was deposited at downstream and the ripples continued moved to downstream of the pier. The maximum scour depth occurred in front of pier nose for all test duration.

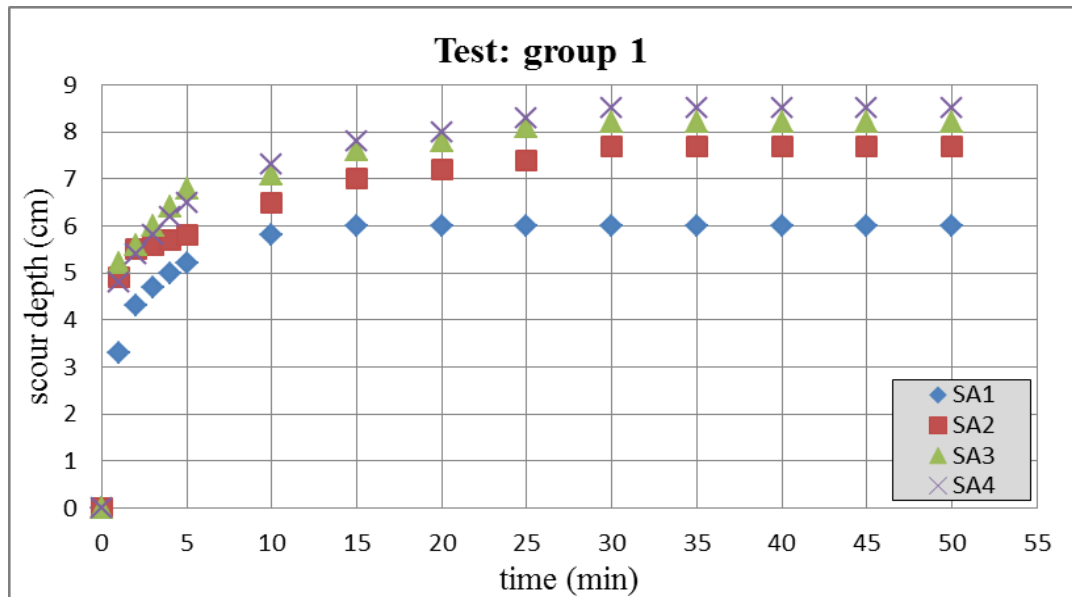


Figure 4.5 Time evolution in scour depth for all test in Group 1

In Figure 4.5, the four test in Group 1 are shown (SA1, SA2, SA3, SA4), it's clear that every test after 35 minutes from test start going to equilibrium condition. SA1 is the first test reached to equilibrium condition after 15 minutes. Figure 4.5 shows very clearly that scour depth increases by increasing discharge for a constant diameter of bridge pier.

4.2.5 Bathymetry and 3-dimensional view of the scoured bed for Group 1 tests

Computer software called Surfer© version (10) was used to sketch the 3D map and bathymetry of the bed for group 1 which include SA1, SA2, SA3, and SA4 for pier diameter of 0.05 m, the data plotted in the Figures 4.6 to 4.10 are given in Appendix A. Figure 4.6 shows 3D map for SA1 test after reaching equilibrium condition. It's shown that there is no depression occurred in upstream but there is a deposition in the downstream of the pier. Figure 4.9 shows maximum depression occurs in upstream of the pier for SA4 test, at downstream of the pier, the sand particles deposited behind the pier with regular shape and extended to the end of test section.

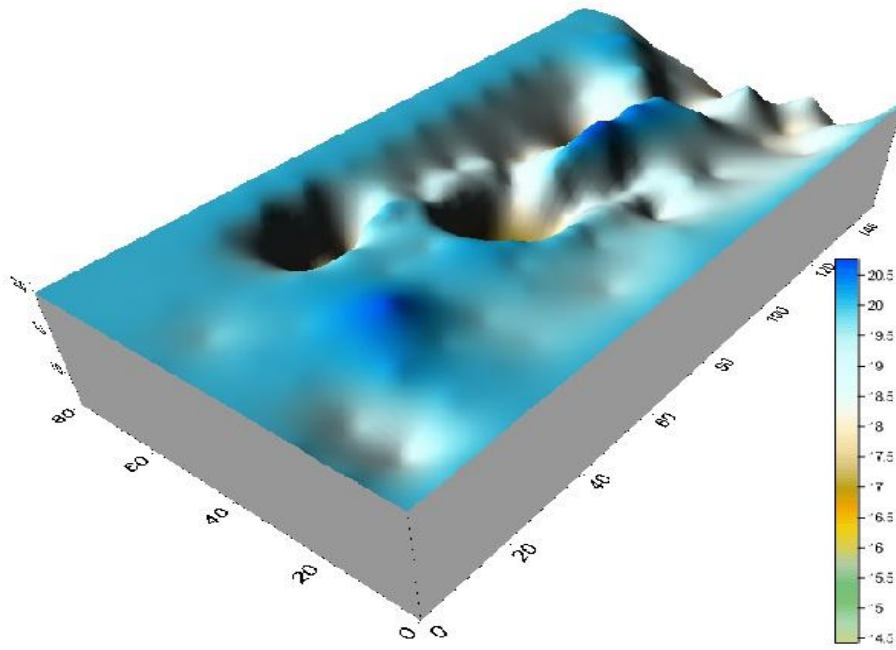


Figure 4.6 3D scour map for SA1

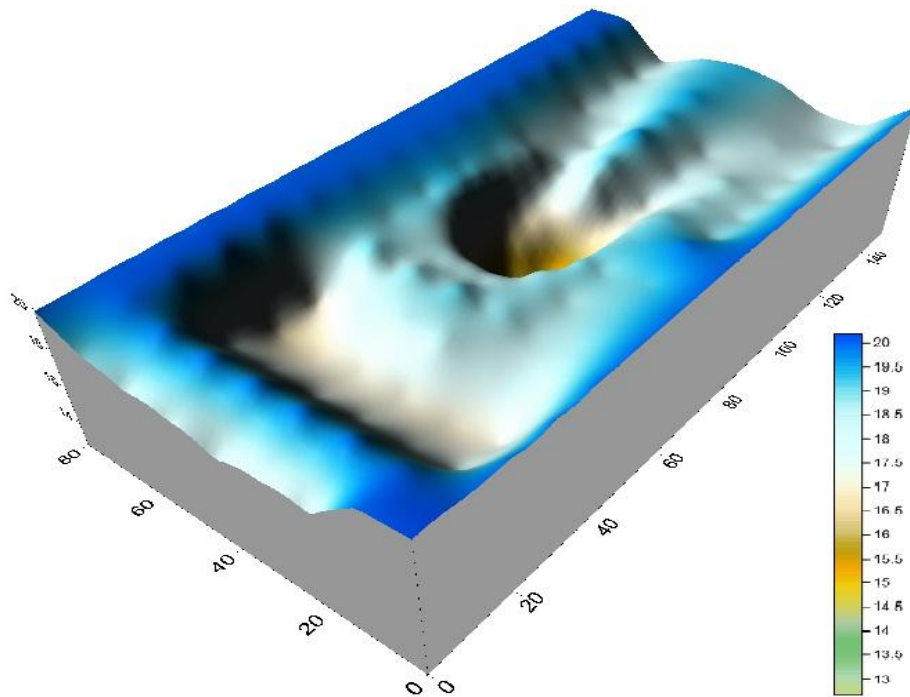


Figure 4.7 3D scour map for SA2

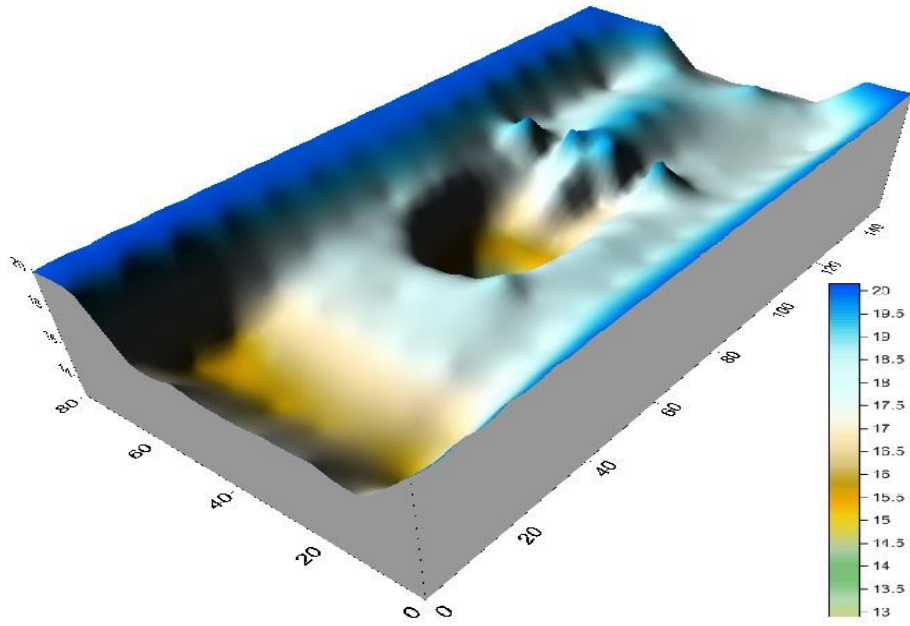


Figure 4.8 3D scour map for SA3

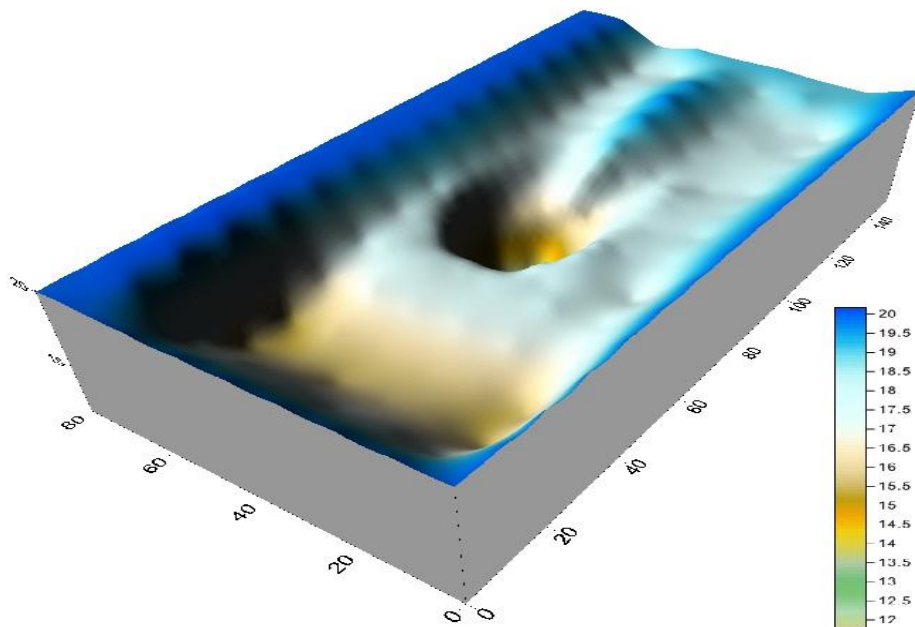


Figure 4.9 3D scour map for SA4

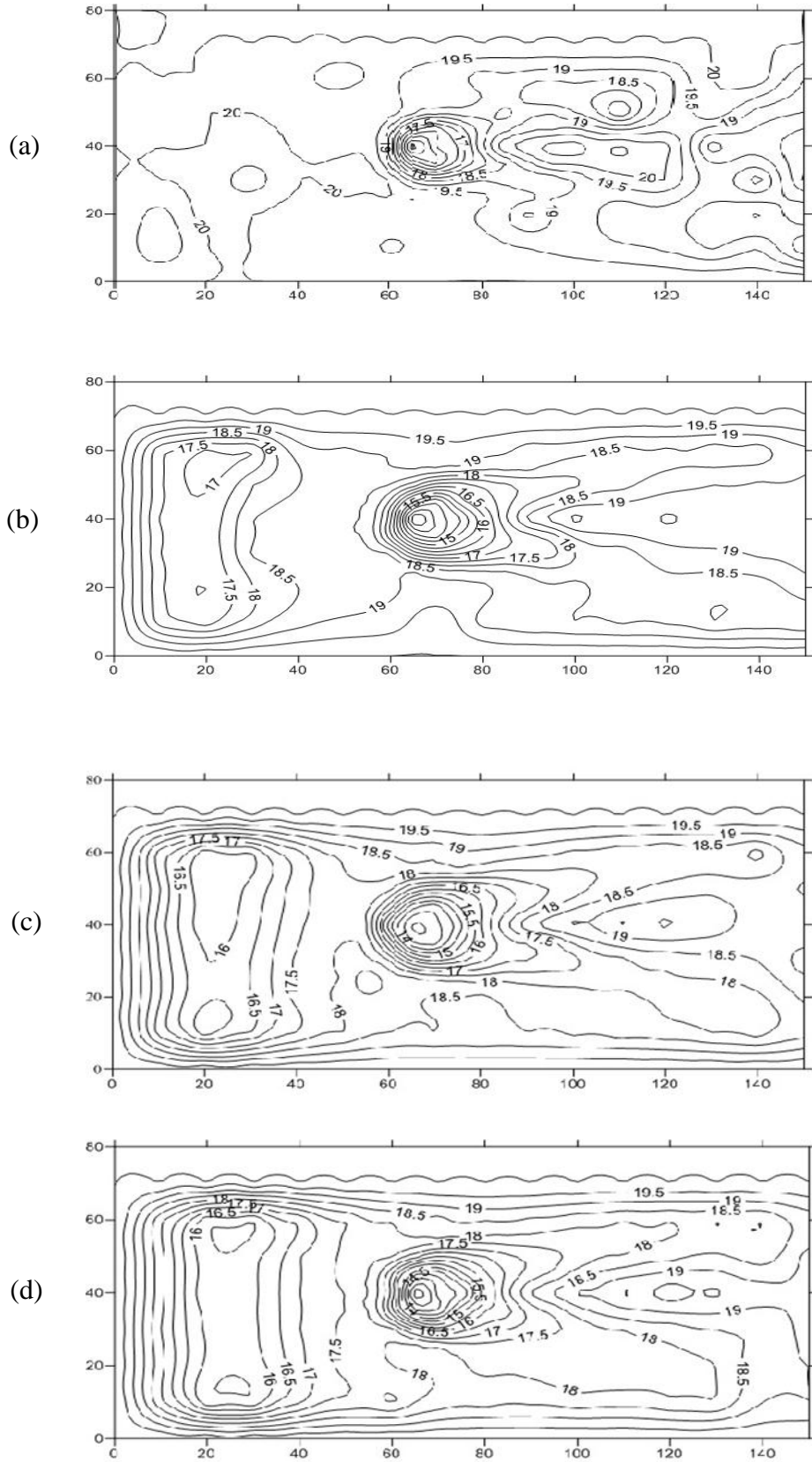
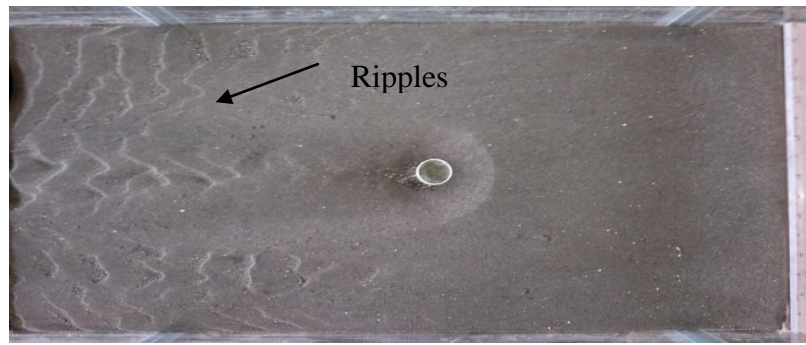


Figure 4.10. Bathymetry of bed for Group 1 tests (scale in cm)

(a) SA1 (b) SA2 (c) SA3 (d) SA4



(a)



(b)

Figure 4.11 Equilibrium scour depth for Group 1 tests, $d=5$ cm
(a) Top view (b) side view

4.3 Local scour depth

Group 2 tests were carried out for a pier diameter of 7.5 cm and 4 different approaching discharges of 6.29 lt/s, 16.6 lit/sec, 22.63 lt/sec, and 25.19 lt/sec. The four tests in Group 2 symbolized with SB1, SB2, SB3, and SB4 as shown in Table 3.1.

4.3.1 Measurement of local scour depth with $d=7.5$ cm and $Q=6.29$ lt/s

Group 2 experiments were done with pier diameter of 7.5 cm at four discharges of the previous Group 1 experiments. Group 2 experiments carried out to study the effect of increasing in pier diameter on local scour depth. Experimental runs are shown in Table 4.5. The scour depth reached to equilibrium condition in 45 minutes with maximum scour depth of 0.061 m.

Table 4.5 Temporal development of scour depth for SB1 ($d= 7.5$ cm, $Q= 6.29$ lt/s)

t (min)	Q (lt/s)	d_{se} (m)	y (m)
1	6.29	0.019	0.025
2	6.29	0.025	0.025
3	6.29	0.032	0.025
4	6.29	0.038	0.025
5	6.29	0.041	0.025
10	6.29	0.053	0.025
15	6.29	0.054	0.025
20	6.29	0.055	0.025
25	6.29	0.056	0.025
30	6.29	0.067	0.025
35	6.29	0.058	0.025
40	6.29	0.06	0.025
45	6.29	0.061	0.025
50	6.29	0.061	0.025

4.3.2 Measurement of local scour depth with $d=7.5$ cm and $Q=16.6$ lt/s

Temporal development of scour depth, are shown in Table 4.6 for experimental run SB2. Local scour reached in equilibrium condition after 25 minutes from the beginning of the test as 0.091 m. The maximum scour depth in SB2 test greater than in SB1 test, due to increasing in approaching discharge.

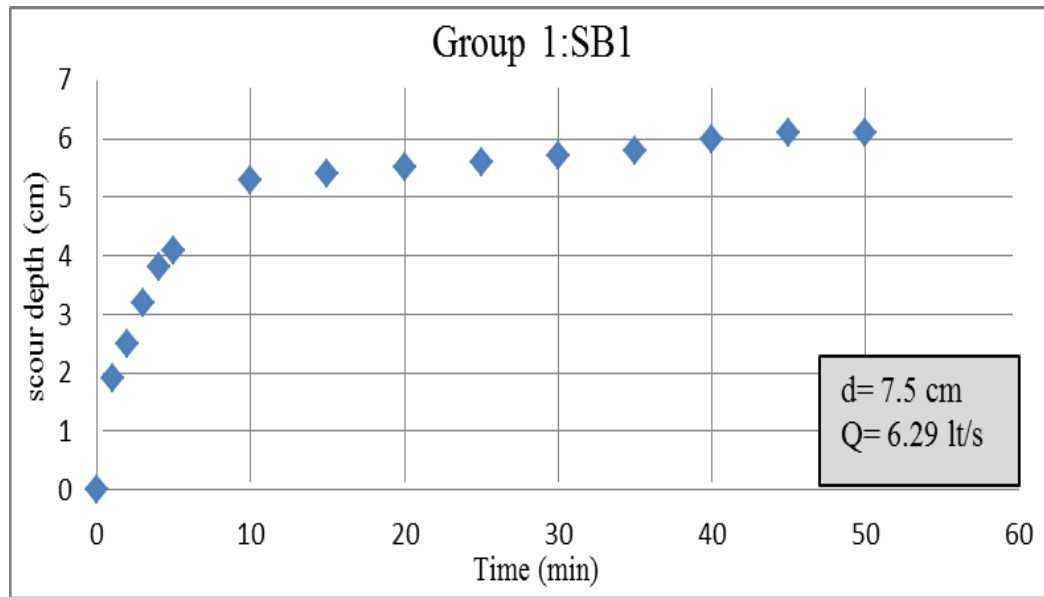


Figure 4.12 Time evolution in scour depth for $d = 7.5 \text{ cm}$, $Q = 6.29 \text{ lt/s}$

Table 4.6 Temporal development of scour depth for SB2 ($d = 7.5 \text{ cm}$, $Q = 16.6 \text{ lt/s}$)

t (min)	Q (lt/s)	d_{se} (m)	y (m)
1	16.6	0.052	0.044
2	16.6	0.064	0.044
3	16.6	0.07	0.044
4	16.6	0.072	0.044
5	16.6	0.074	0.044
10	16.6	0.078	0.044
15	16.6	0.083	0.044
20	16.6	0.085	0.044
25	16.6	0.091	0.044
30	16.6	0.091	0.044
35	16.6	0.091	0.044
40	16.6	0.091	0.044

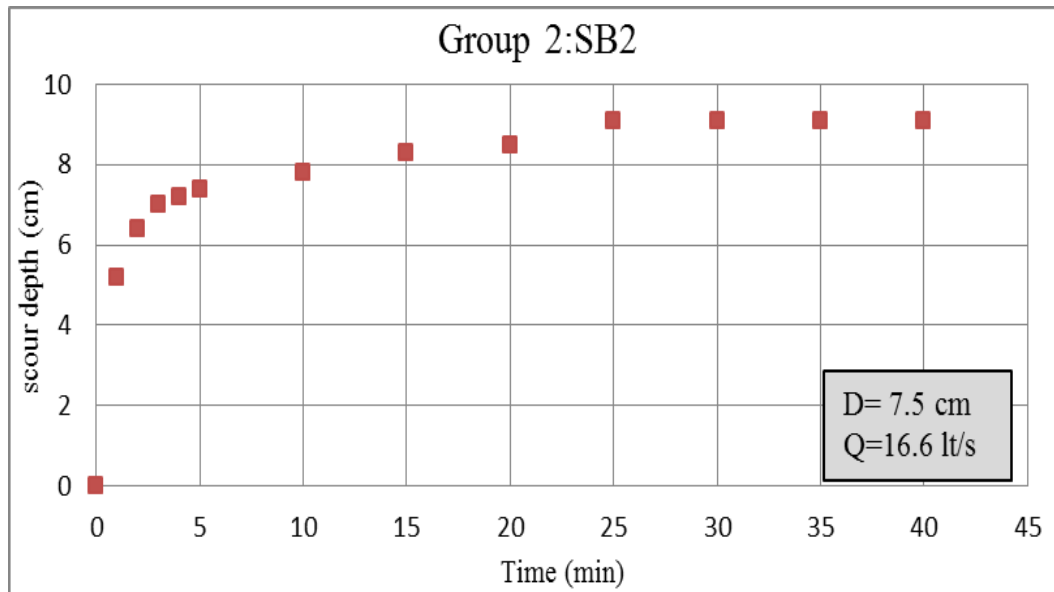


Figure 4.13 Time evolution in scour depth for $d=7.5\text{cm}$, $Q=16.6\text{ lt/s}$

4.3.3 Measurement of local scour depth with $d=7.5\text{ cm}$ and $Q=22.63\text{ lt/s}$

In this test, the pier diameter of 7.5 cm which tested with 22.63lt/s of discharge as shown in Table 4.7 with flow depth of 0.054 m. After running the test, during the first 5 minutes the depth of scour measured immediately and it's noted that the change in scour depth between two run was larger than the change in scour depth was measured after 15 minutes, the reason it was some particles of sediment move from upstream of the pier with flow direction toward the scour hole and fall in it, some of this particles due to vortices its move up out of scour hole and rolling toward the downstream of the pier, with over time, this process make the change in scour depth small between two run.

Table 4.7 Temporal development of scour depth for SB3(d=7.5cm, Q=22.63 lt/s)

t (min)	Q (lt/s)	d _{se} (m)	y (m)
1	22.63	0.055	0.054
2	22.63	0.065	0.054
3	22.63	0.068	0.054
4	22.63	0.075	0.054
5	22.63	0.077	0.054
10	22.63	0.086	0.054
15	22.63	0.09	0.054
20	22.63	0.093	0.054
25	22.63	0.096	0.054
30	22.63	0.097	0.054
35	22.63	0.097	0.054
40	22.63	0.097	0.054

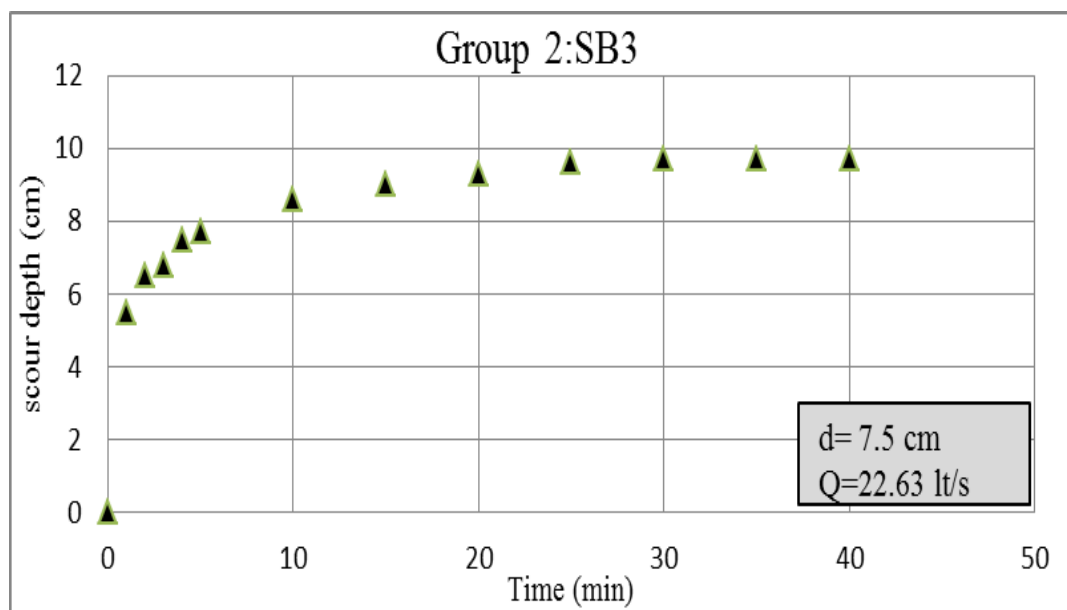


Figure 4.14 Time evolution in scour depth for d= 7.5cm, Q= 22.63 lt/s

4.3.4 Measurement of local scour depth with $d=7.5$ cm and $Q=25.19$ lt/s

In this test, the pier diameter of 7.5 cm was tested with discharge of 25.19 lt/s. Table 4.8 shows data of temporal development of scour depth for SB4 test, after equilibrium condition reached with maximum scour depth of 0.105 m and the test stopped in 55 minutes from test start.

Table 4.8 Temporal development of scour depth for SB3 ($d=7.5$ cm, $Q=25.19$ lt/s)

t (min)	Q (lt/s)	d_{se} (m)	y (m)
1	25.19	0.057	0.058
2	25.19	0.064	0.058
3	25.19	0.07	0.058
4	25.19	0.072	0.058
5	25.19	0.078	0.058
10	25.19	0.087	0.058
15	25.19	0.095	0.058
20	25.19	0.098	0.058
25	25.19	0.099	0.058
30	25.19	0.10	0.058
35	25.19	0.101	0.058
40	25.19	0.102	0.058
45	25.19	0.103	0.058
50	25.19	0.105	0.058
55	25.19	0.105	0.058

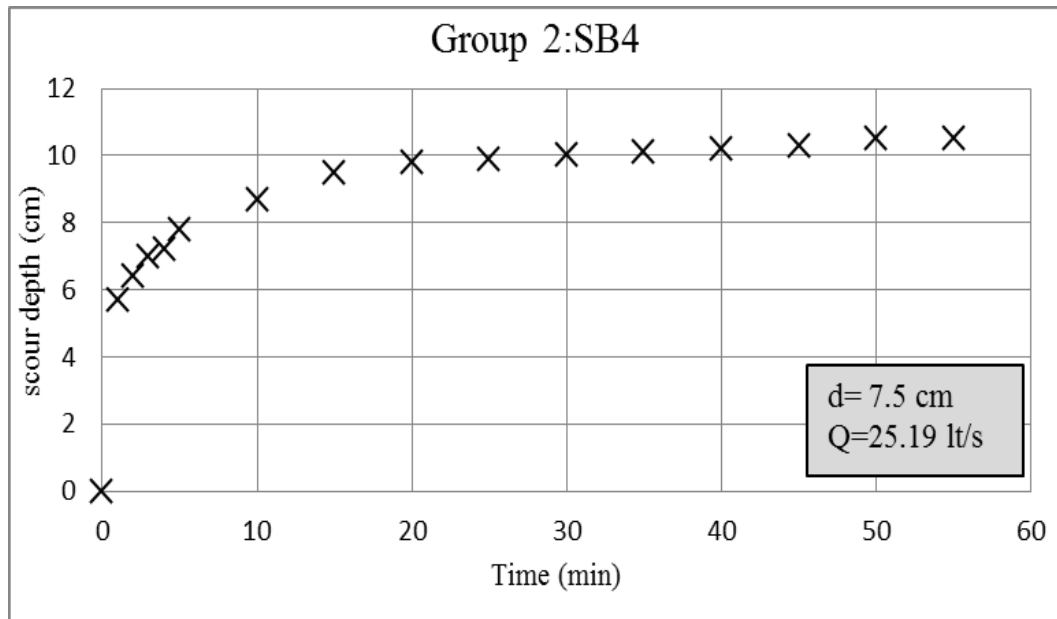


Figure 4.15 Time evolution in scour depth for $d=7.5\text{cm}$, $Q= 25.19\text{ lt/s}$

Figure 4.15 shows development in scour depth with respect to time for SB4 test. The results of SB4 test indicate that maximum scour depth for this test greater than maximum scour depth for SB1, SB2, and SB3 tests; Figure 4.16 shows the comparison between four tests for Group 2. In Group 2 tests, there are elements effects on local scour depth; by make one of these elements constant (in case of Group 2 the pier diameter is constant) the results indicate that discharge and time was effected on scour depth, with increasing in time the local scour depth increases and with increasing in discharge the maximum scour depth increases.

4.3.5 Bathymetry and 3-dimensional view of the scoured bed for Group 2 tests

The 3D map and contour profile map of the scour hole for Group 2 tests which include SB1, SB2, SB3, and SB4 for pier diameter of 7.5 cm. The data plotted in Figures started from 4.18 to 4.25 are given in Appendix A. As shown in Figure 4.18, SB1 test in lower discharge, the erosion in surface of the sediment at upstream of pier was smaller than in other tests. In Figure 4.19, it's seen there is a depression in

upstream level and also there is a formation of dune in downstream level. Figure 4.20 and Figure 4.21 show the distribution in bed level for SB3 test and SB4 test, there are no large changes in two tests if one makes a comparison between them, the reason of this case is the discharge for SB3 test and SB4 test are close to each other.

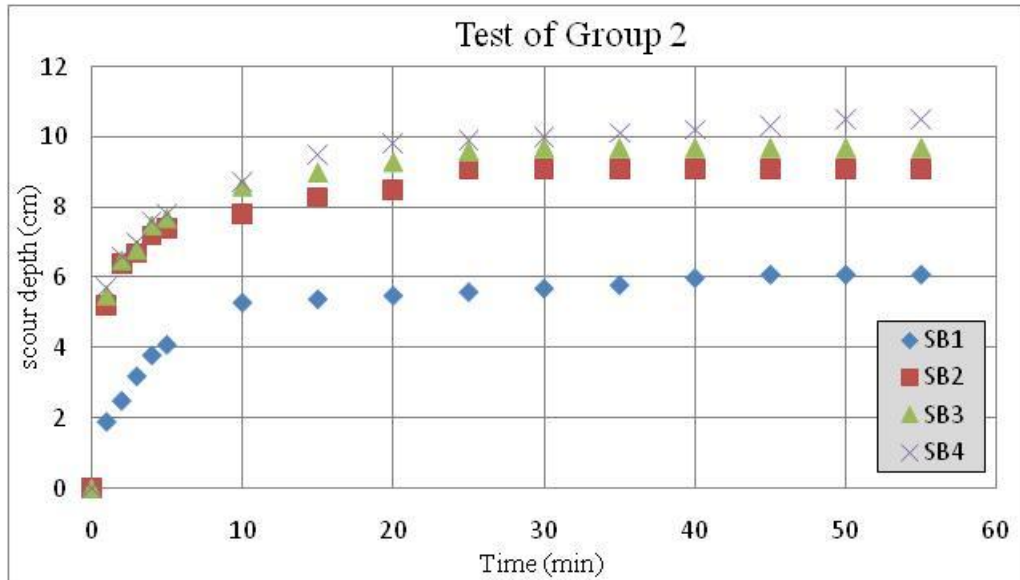


Figure 4.16 Time evolution in scour depth for all test in Group 2



Figure 4.17 Equilibrium scour depth for Group 2 tests ($d=7.5\text{cm}$)

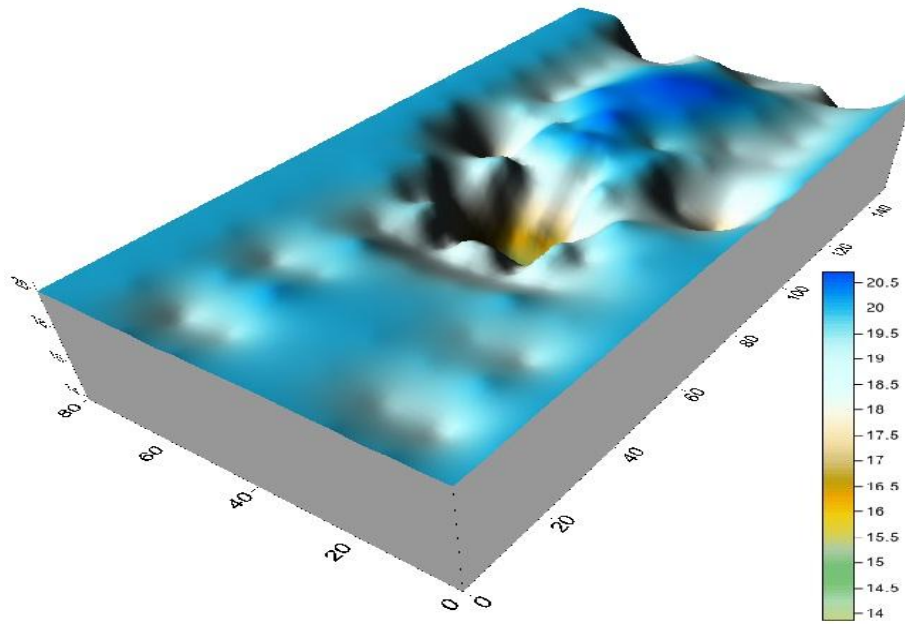


Figure 4.18 3D scour map for SB1

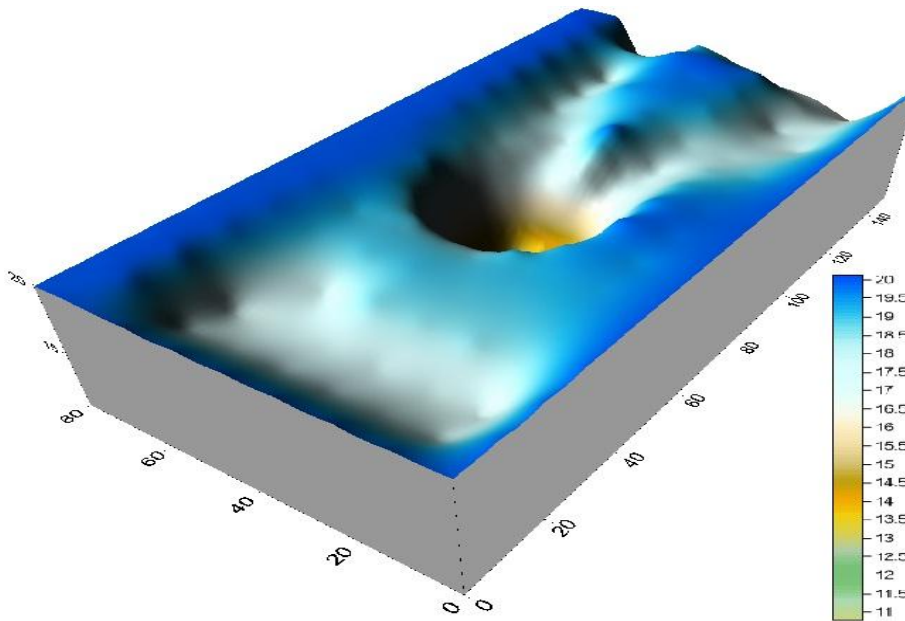


Figure 4.19 3D scour map for SB2

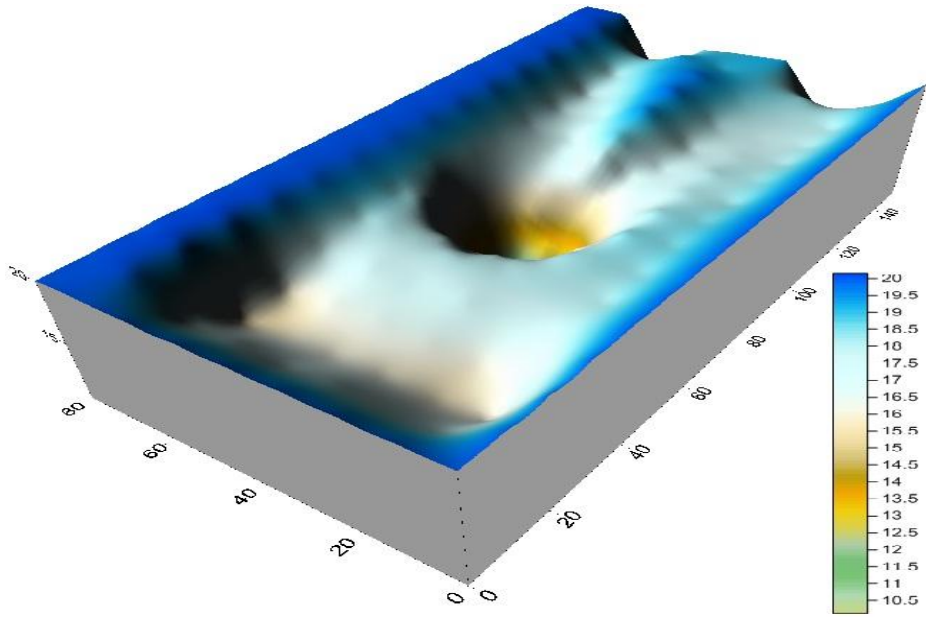


Figure 4.20 3D scour map for SB3

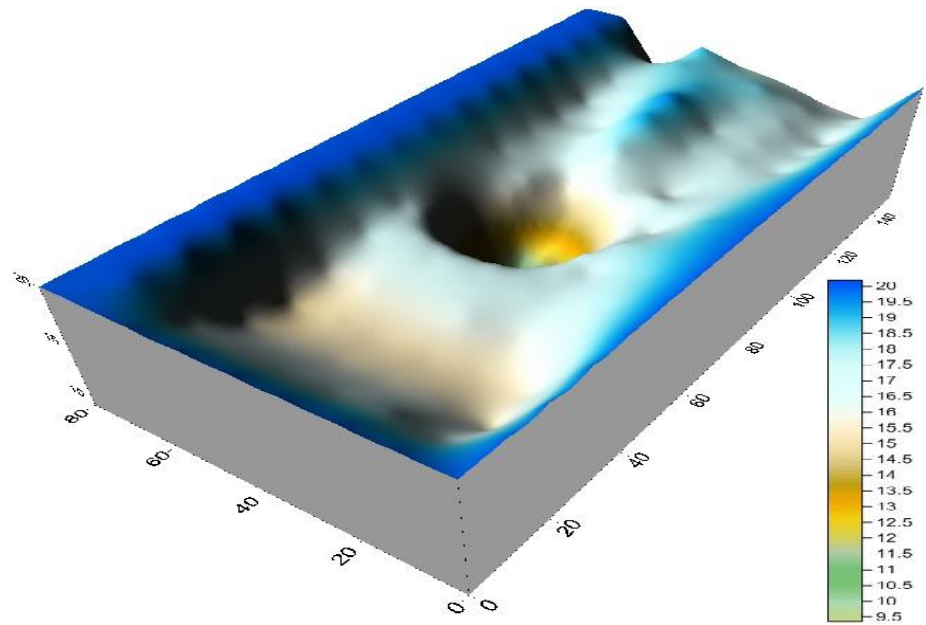


Figure 4.21 3D scour map for SB4

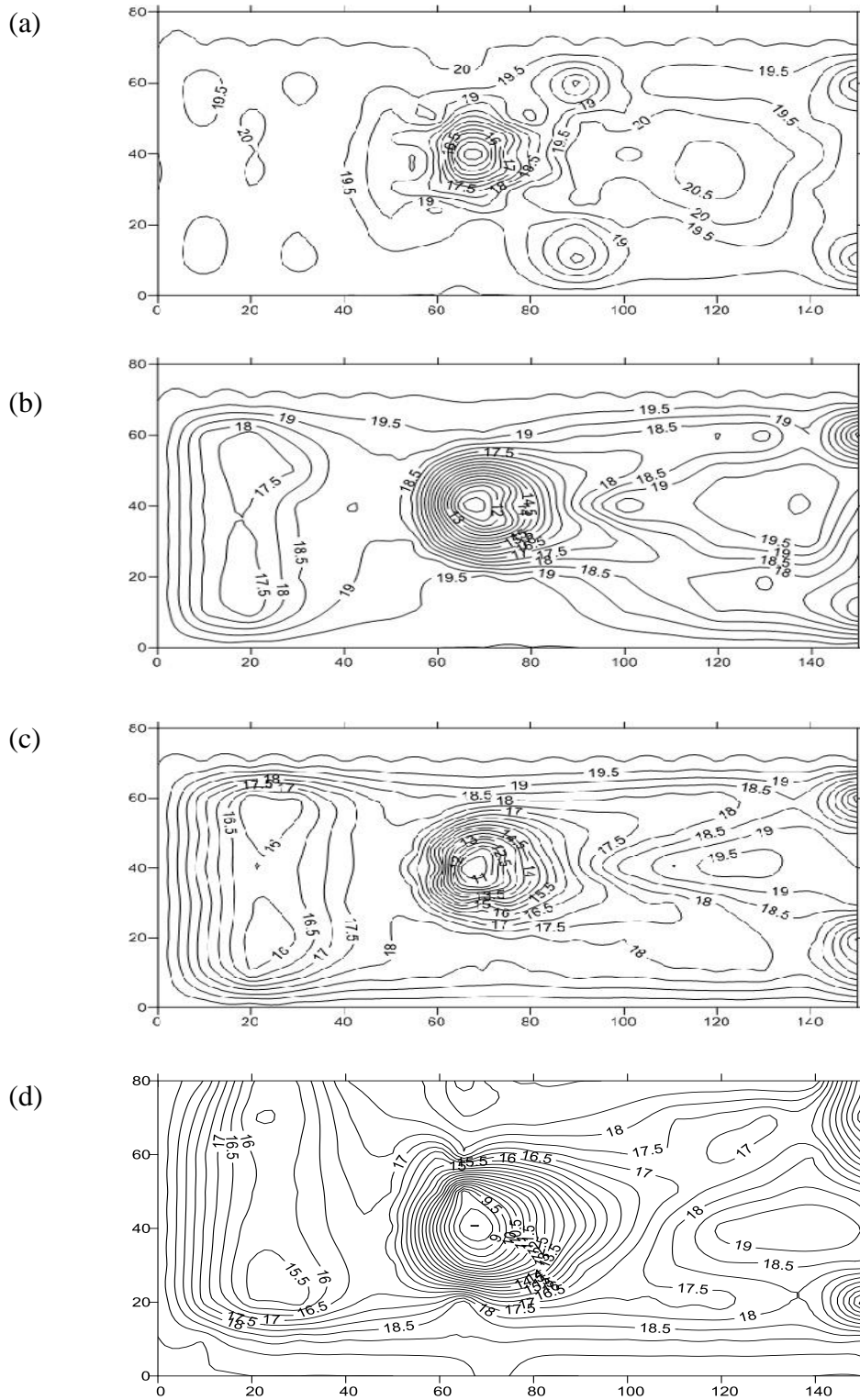


Figure 4.22 Bathymetry of the bed for Group 2 tests (scale in cm)

(a) SB1 (b) SB2 (c) SB3 (d) SB4

4.3.6 Comparison between Group1 and Group 2 results

The comparison in temporal development of local scour depth between Group 1 and Group 2 tests, as shown in Figure 4.23, the results of SA1 and SA4 tests combined with the results of SB1 and SB4 tests to see the change in maximum scour depth with increasing in time. As shown in Figure 4.23, in 10 minutes from the beginning of the tests, there are differences in scour depth for all results, while SA1 test and SB1 test are tested in same discharge (minimum discharge) and it's noted that after 30 minutes there is a convergence between SA1 test and SB1 test. The test of SA4 and SB4 that was tested with the same discharge (maximum discharge) it's clear that the maximum scour depth in SB4 test greater than SA4 test. The results in Figure 4.23 show that there is an effect of pier diameter to maximum scour depth. In summary, increases in pier diameter with constant approaching discharges, the maximum scour depth will increase.

4.3.7 Longitudinal scour profile for Group 2 tests

The longitudinal scour profile in Group 2 was plotted in Figure 4.27. The data was measured along the centerline of the flume and the pier was installed at the centerline in longitudinal direction with 65 cm away from the upstream. Figure 4.24 shows that the four tests for Group 2 started from SB1 to SB4, the surface was measured after reaching to equilibrium condition for every test, the maximum scour depth, it is the deepest portion formed at upstream face of the pier, at downstream of the pier the mound and ripples are formed but in another way there are erosions in upstream of the pier. The maximum depth of erosions noted in SB4 test as shown in Figure 4.24. The data plotted in Figure 4.27 are given in Appendix A.

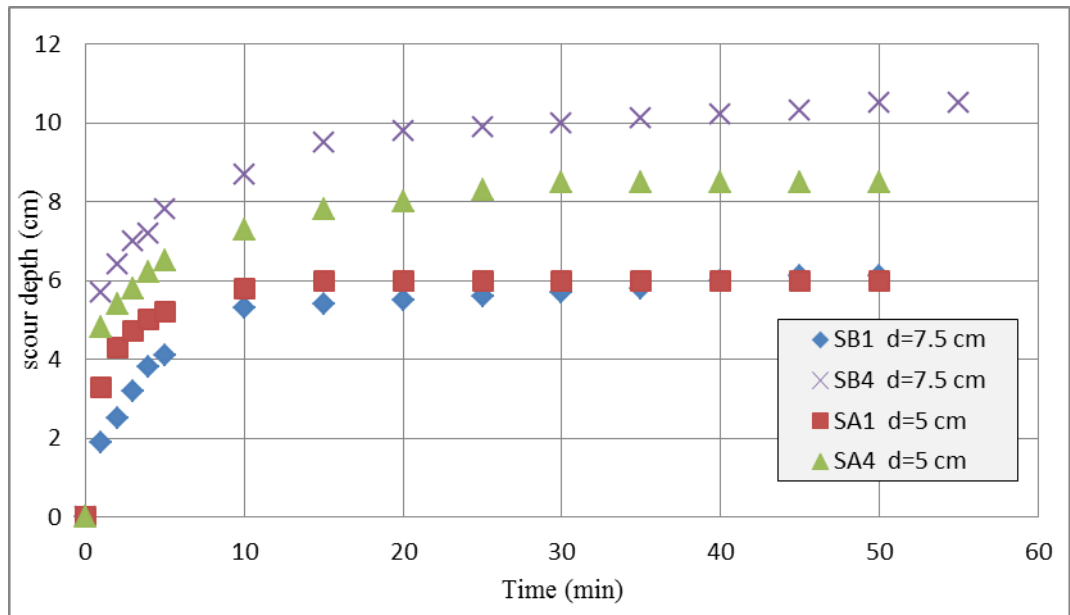


Figure 4.23 Comparison of the temporal development of maximum scour depth between Group 1 and Group 2 tests

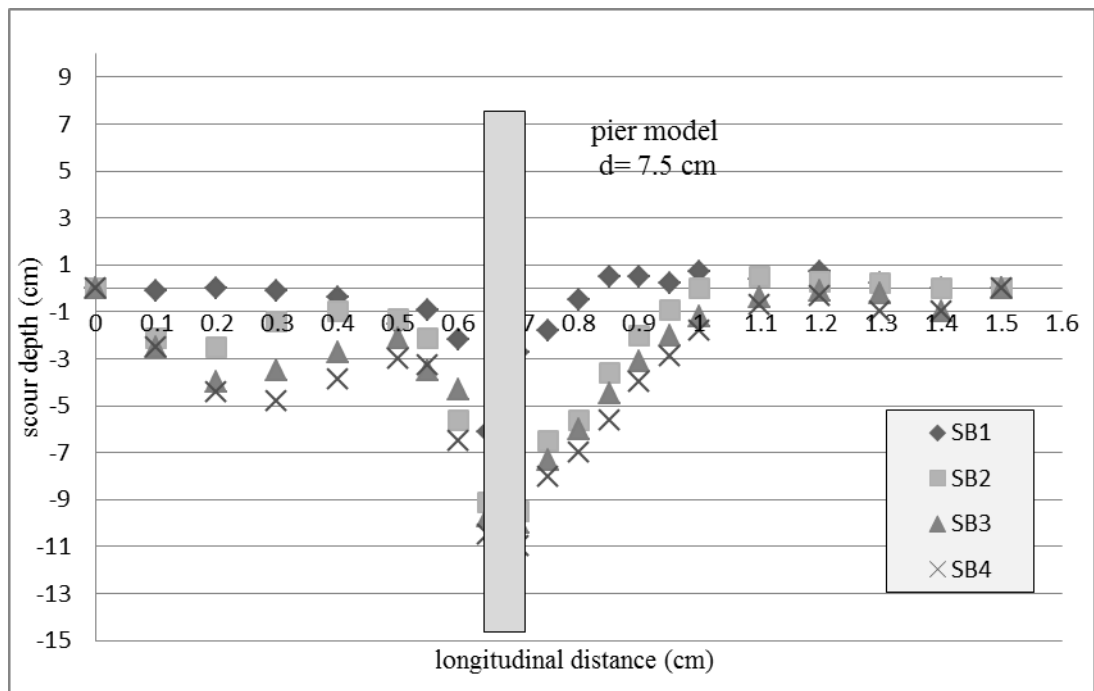


Figure 4.24 Longitudinal scour profile for Group 2 tests

4.4 Local scour depth

Group3 tests were carried out for a pier diameter of 11.1cm and 4 different approaching discharges of 6.29 lt/s, 16.6 lt/s, 22.63 lt/s, and 25.19 lt/s. The four tests in Group 2 are symbolized with SC1, SC2, SC3, and SC4 as shown in Table 3.1.

4.4.1 Measurement of local scour depth with $d=11.1$ cm and $Q=6.29$ lt/s

In this test, 11.1 cm of pier diameter was used; Table 4.9 shows the time variation of local scour depth for 6.29 lt/s of discharge and flow depth of 0.025 m. Equilibrium condition reached after 30 minutes from the beginning of the test with a maximum scour depth of 0.064 m.

Table 4.9 Temporal development of scour depth for SC1 ($d=11.1$ cm, $Q=6.29$ lt/s)

t (min)	Q (lt/s)	d_{se} (m)	y (m)
1	6.29	0.010	0.025
2	6.29	0.020	0.025
3	6.29	0.025	0.025
4	6.29	0.028	0.025
5	6.29	0.033	0.025
10	6.29	0.052	0.025
15	6.29	0.060	0.025
20	6.29	0.061	0.025
25	6.29	0.063	0.025
30	6.29	0.064	0.025
35	6.29	0.064	0.025
40	6.29	0.064	0.025

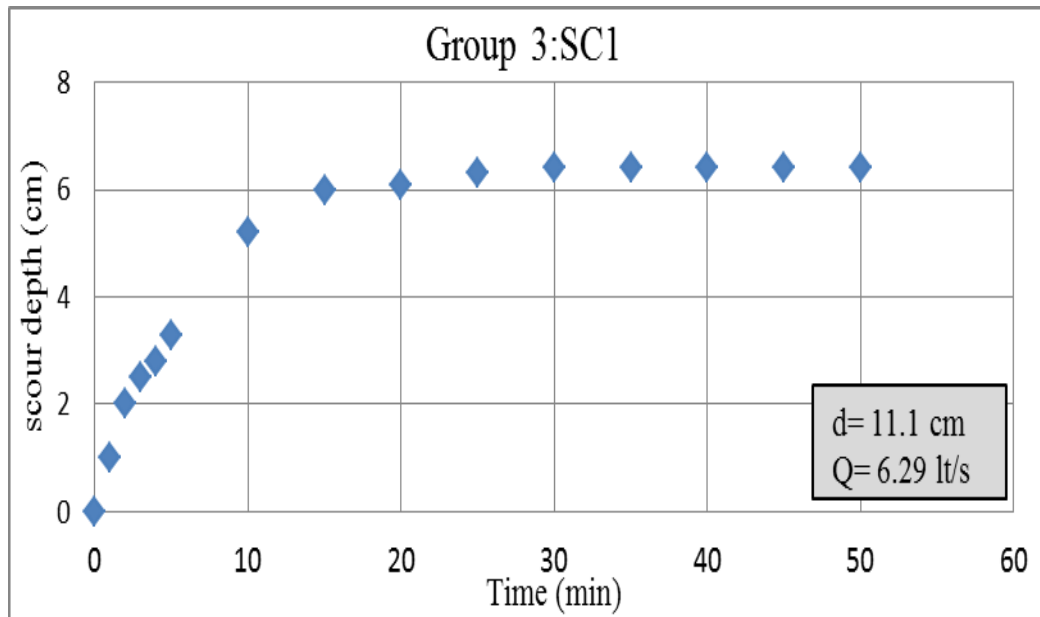


Figure 4.25 Time evolution in scour depth for $d=11.1\text{ cm}$, $Q= 6.29\text{ lt/s}$

Figure 4.25 shows development in local scour depth depending on different time for test SC1. Maximum scour depth for this test reached to 0.064 m, SA1 and SB1 tests have same discharge of 6.29 lt/s with different pier diameter. It is very clear that there are changes in maximum scour depth for the three tests. Among the three tests, biggest maximum scour depth located in SC1, with increasing in pier diameter the maximum scour depth increases with constant discharge.

4.4.2 Measurement of local scour depth with $d=11.1\text{ cm}$ and $Q =16.6\text{ lt/s}$

Second test in Group 3 includes pier diameter of 11.1cm and discharge of 16.6 lt/s with 0.044 m of flow depth. Table 4.10 shows data for temporal development of local scour depth for SC2 test.

Table 4.10 Temporal development of scour depth for SC2 (d=11.1cm, Q=16.6 lt/s)

t (min)	Q (lt/s)	d _{se} (m)	y (m)
1	16.6	0.06	0.044
2	16.6	0.074	0.044
3	16.6	0.081	0.044
4	16.6	0.086	0.044
5	16.6	0.089	0.044
10	16.6	0.097	0.044
15	16.6	0.104	0.044
20	16.6	0.108	0.044
25	16.6	0.109	0.044
30	16.6	0.11	0.044
35	16.6	0.111	0.044
40	16.6	0.112	0.044
45	16.6	0.112	0.044
50	16.6	0.112	0.044

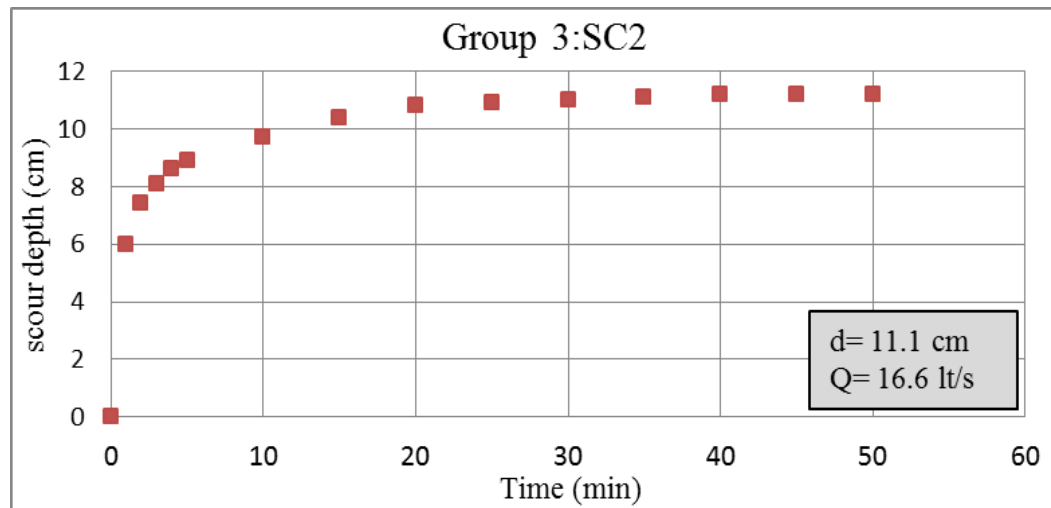


Figure 4.26 Time evolution in scour depth for d=11.1cm, Q= 16.6 lt/s

Development of scour depth for test of SC2 is shown in Figure 4.26, with approaching discharge of 16.6 lt/s. It is seen from Figure 4.26 the maximum scour

depth for the test of SC2 reached to 0.112 m. It is clear that, increasing in discharge the maximum scour depth will increase with constant pier diameter.

4.4.3 Measurement of local scour depth with $d=11.1$ cm and $Q=22.63$ lt/s

Third test in Group 3 includes pier diameter of 11.1 cm and discharge of 22.63 lt/s. Table 4.11 shows data for temporal development of scour depth of SC3 test, the flow depth located about 0.054 m above sand bed.

Table 4.11 Temporal development of scour depth for SC3 ($d=11.1$ cm, $Q=22.63$ lt/s)

t (min)	Q (lt/s)	d_{se} (m)	y (m)
1	22.63	0.065	0.054
2	22.63	0.078	0.054
3	22.63	0.085	0.054
4	22.63	0.088	0.054
5	22.63	0.095	0.054
10	22.63	0.107	0.054
15	22.63	0.11	0.054
20	22.63	0.112	0.054
25	22.63	0.113	0.054
30	22.63	0.116	0.054
35	22.63	0.117	0.054
40	22.63	0.117	0.054
45	22.63	0.117	0.054
50	22.63	0.117	0.054

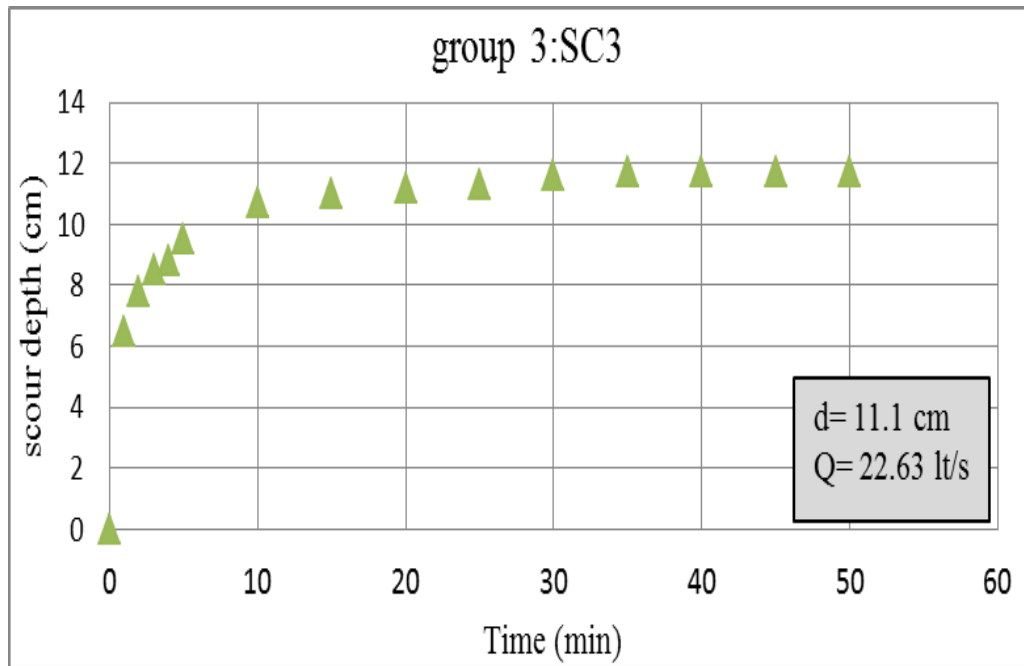


Figure 4.27 Time evolution in scour depth for $d=11.1\text{ cm}$, $Q= 22.63\text{lt/s}$

For SC3 test, there is an increase in maximum scour depth by comparing it with maximum scour depth for SC2 test. Figure 4.27 shows that SC3 test reached to equilibrium condition in 35 minutes, which means the time of equilibrium condition decreases in SC3 test if it is compared with SC2 test.

4.4.4 Measurement of local scour depth with $d=11.1\text{ cm}$ and $Q=25.19\text{ lt/s}$

Final test in Group 3 were carried out with pier diameter of 11.1 cm, and a discharge of 25.19 lt/s. Table 4.12 shows data for temporal development of scour depth for SC4, the flow depth located about 0.058 m above sand bed.

Table 4.12 Temporal development of scour depth for SC4 (d=11.1cm, Q=25.19 lt/s)

t (min)	Q (lt/s)	d _{se} (m)	y (m)
1	25.19	0.065	0.058
2	25.19	0.082	0.058
3	25.19	0.09	0.058
4	25.19	0.093	0.058
5	25.19	0.097	0.058
10	25.19	0.108	0.058
15	25.19	0.115	0.058
20	25.19	0.116	0.058
25	25.19	0.117	0.058
30	25.19	0.119	0.058
35	25.19	0.119	0.058
40	25.19	0.119	0.058

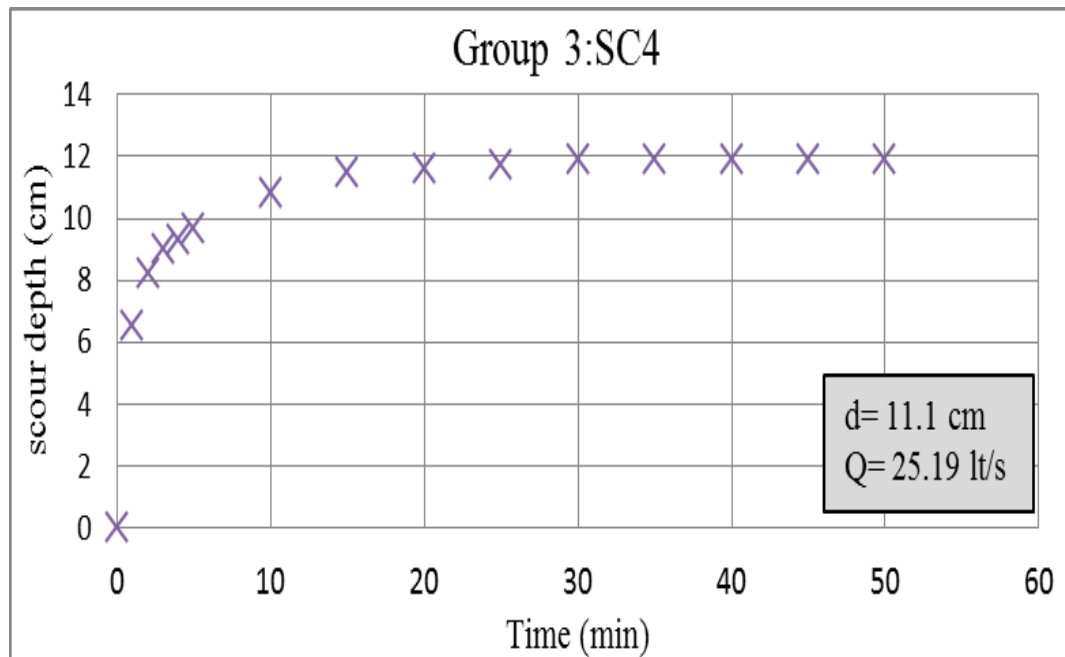


Figure 4.28 Time evolution in scour depth for d=11.1cm, Q= 25.19 lt/s

For the test of SC4, were carried with maximum discharge of 25.19 lt/s. Maximum scour depth in SC4 test reached to 0.119 m, by comparing this result with maximum scour depth for SA4 and SB4 tests, shows that maximum scour depth in SC4 test greater than in SA4 and SB4 tests (Figure 4.29).

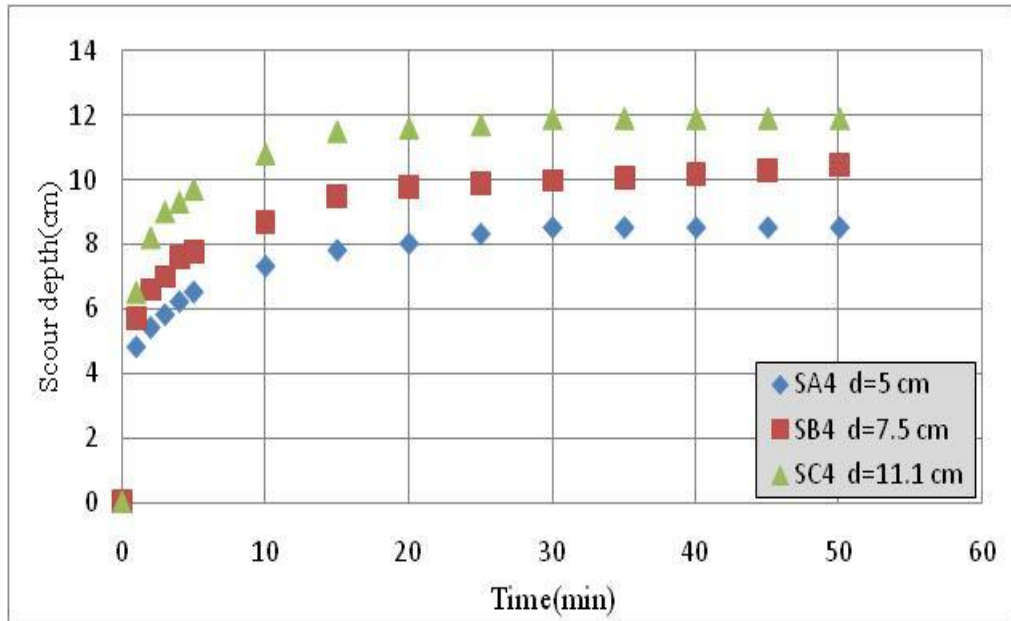


Figure 4.29 Temporal variation of scour depth in SA4, SB4, and SC4 tests

It is seen from Figure 4.29 that there are variation in scour depth in 10 minutes. It's clear from Figure 4.29 that when pier diameter increases the maximum scour depth will increase with the same approaching discharge. Figure 4.30 shows pier bridge model in Group 3 with pier diameter of 11.1 cm, it is seen that there are ripples occur at downstream of pier, because of vortices around the bridge pier model.

4.4.5 Bathymetry and 3-dimensional view of the scoured bed for Group 3 tests

The 3D map and contour profile map of the scour test Group 3 that includes SC1, SC2, SC3, and SC4 for pier diameter of 11.1 cm. The data plotted in Figures started from 4.31 to 4.35 are given in Appendix A. As shown in Figure 4.31, SC1 test in lower discharge, the erosion in surface of the sediment at upstream of pier was

smaller than in other tests. It is seen from Figure 4.34 that there is a depression in upstream level and also there is a formation of dune in downstream level. Figure 4.35 and 4.36 show the distribution in bed level for SC3 and SC4 tests, there are no large changes in two tests if one makes a comparison between them.



Figure 4.30 Experimental work shows pier for group 3 ($d=11.1\text{cm}$)

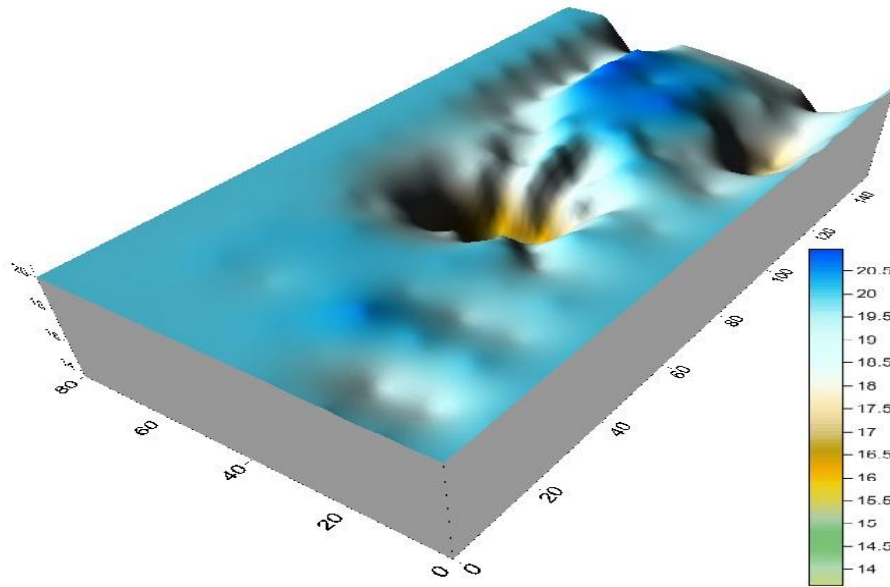


Figure 4.31 3D scour map for SC1

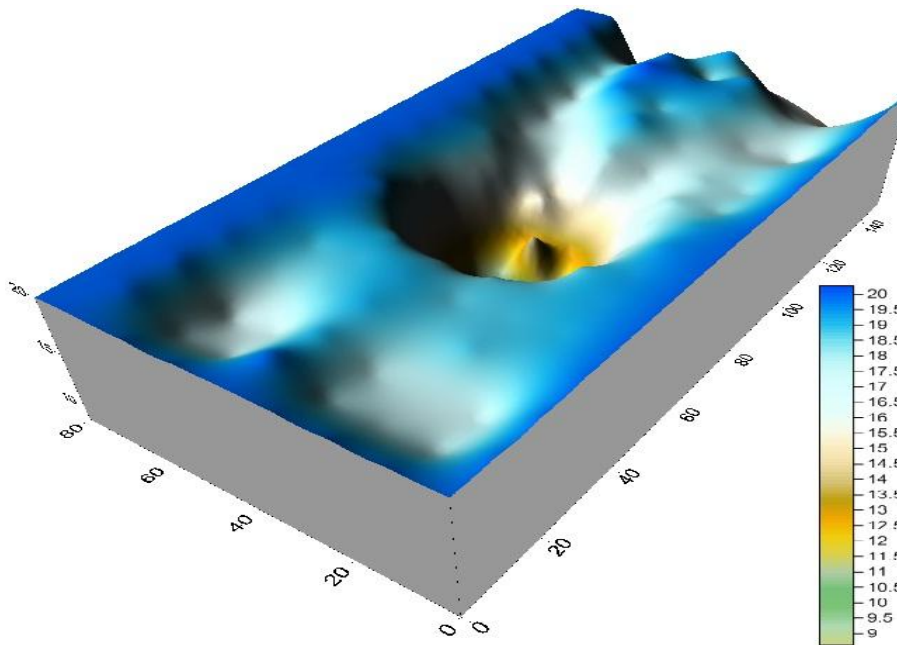


Figure 4.32 3D scour map for SC2

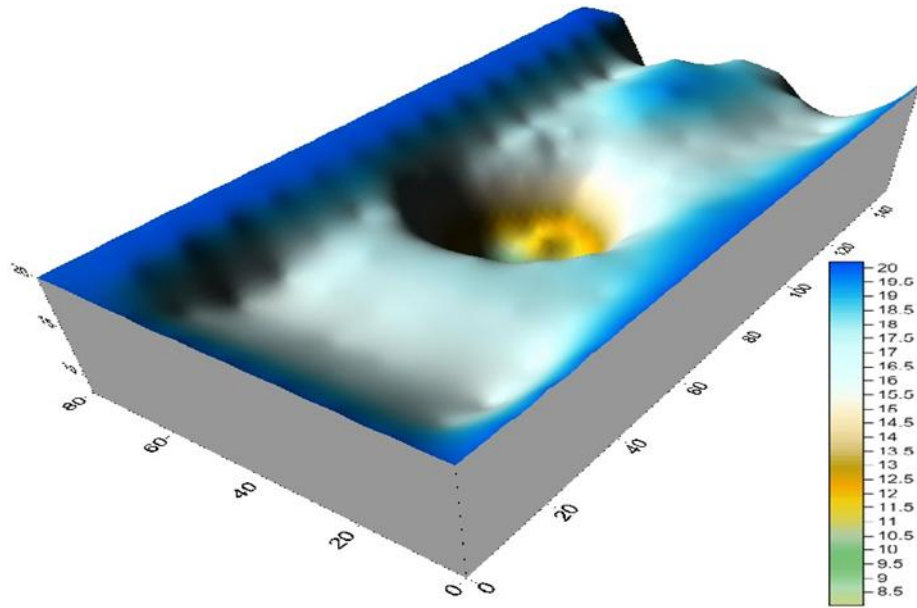


Figure 4.33 3D scour map for SC3

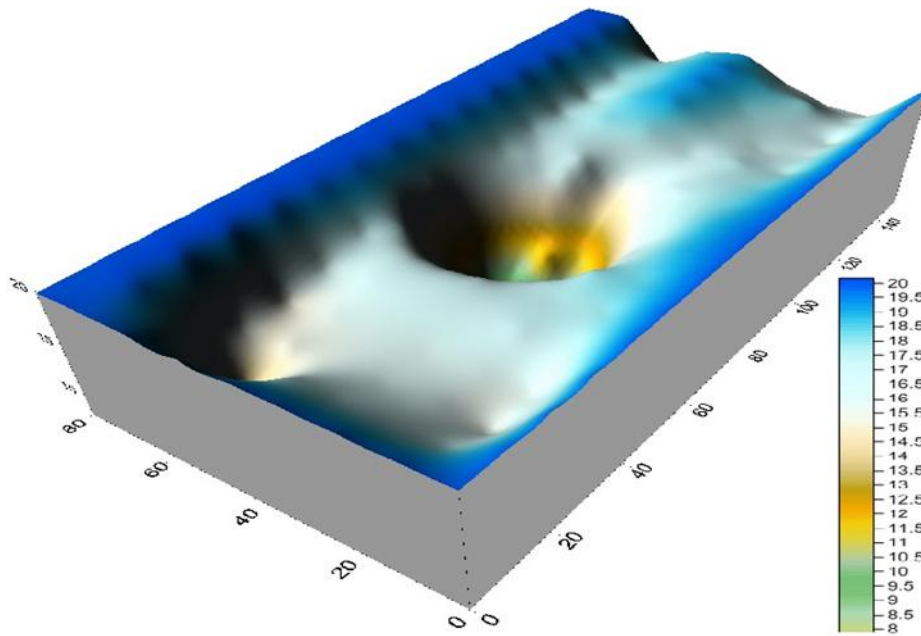


Figure 4.34 3D scour map for SC4

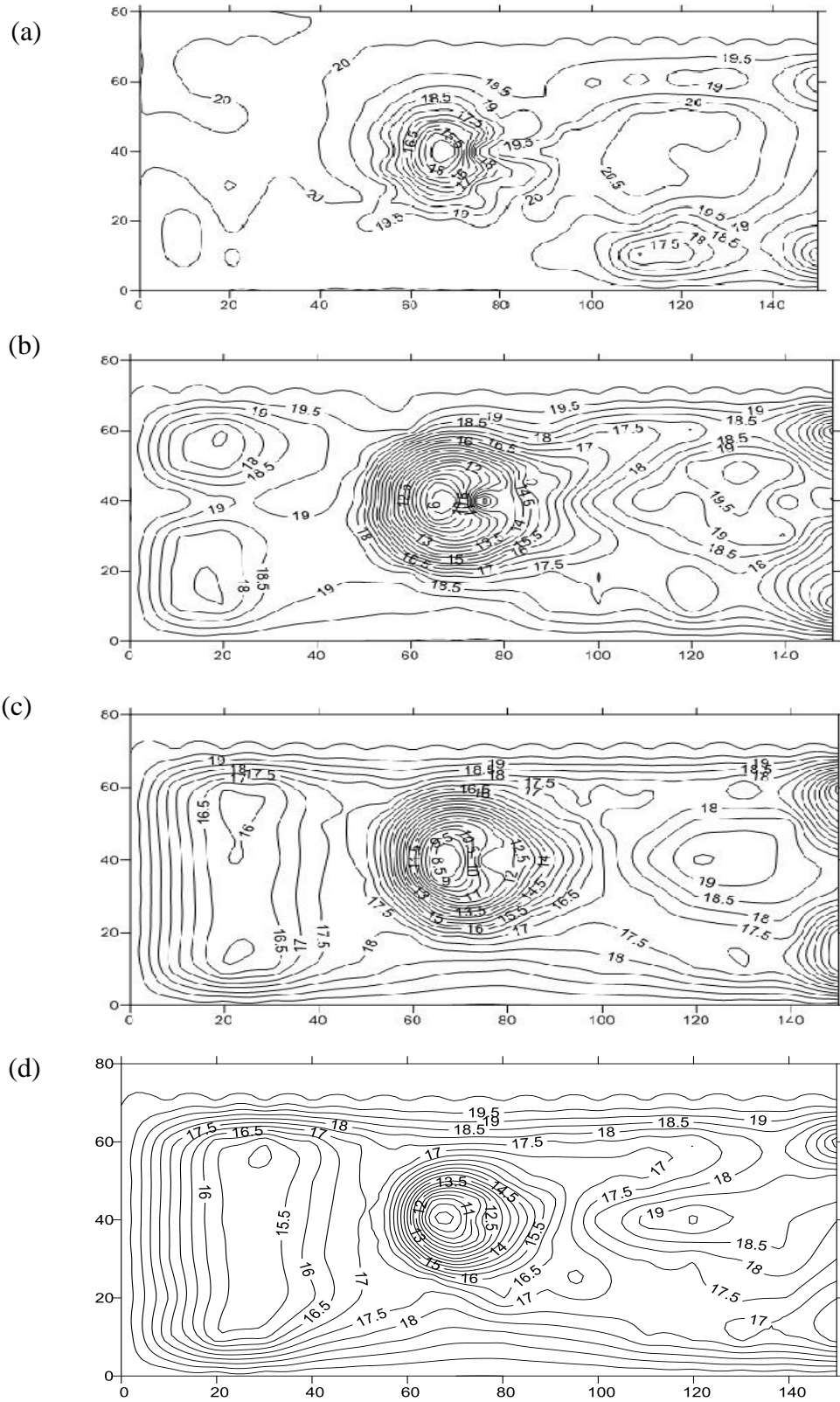


Figure 4.35 Bathymetry of the bed for Group 3 tests (scale in cm)

(a) SC1 (b) SC2 (c) SC3 (d) SC4

4.4.6 Comparison in results between Group2 and Group3 results

The comparison in temporal development of local scour depth between Group 2 and Group 3 are shown in Figure 4.36. The results of SB1 (minimum discharge) and SB4 (maximum discharge) combined with results of SC1 (minimum discharge) and SC4 (maximum discharge). As shown in Figure 4.36, in 10 minutes from the start of experiments there are difference in scour depth, while SA1 and SB1 are tested in same discharge (minimum discharge), and it's noted that after 30 minutes there is a convergence between SA1 and SB1 tests. SA4 and SB4 were tested with same discharge (maximum discharge), it's clear that the maximum scour depth variation in two tests, where the maximum scour depth in SC4 greater than in SB4. The result in Figure 4.36 shows that there is an effect of pier diameter on maximum scour depth. Whenever the pier diameter increases with constant discharge the maximum scour depth will increase.

4.4.7 Longitudinal scour profile for Group 3 tests

The longitudinal scour profile in Group 3 was plotted in Figure 4.37; the data was measured along the centerline of the flume where the pier installed at the centerline in longitudinal direction with 65 cm away from upstream. Figure 4.37 shows the four tests for Group 3 started from SC1 to SC4. At downstream of the pier the mound and ripples are formed, on the other hand erosions occurred in upstream of the pier. The maximum depth of erosions is occurred in SB4 as shown in Figure 4.37. The data plotted in Figure 4.37 are given in Appendix A. The scour profile for each test measured after the test reached to equilibrium condition.

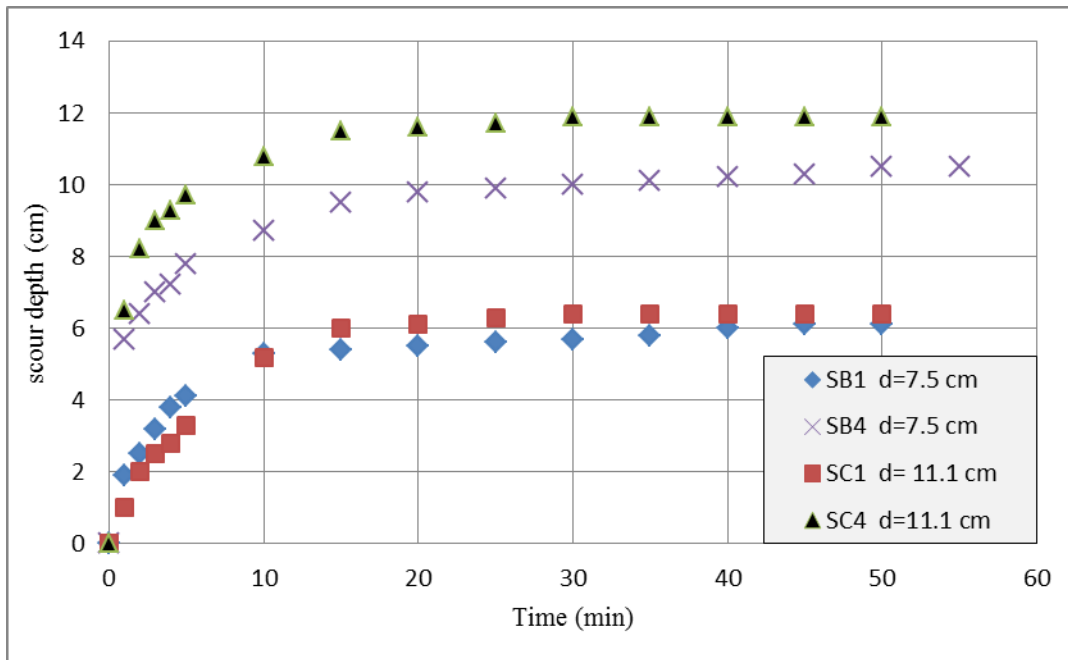


Figure 4.36 Comparison of the temporal development of maximum scour depth between Group 2 and Group 3

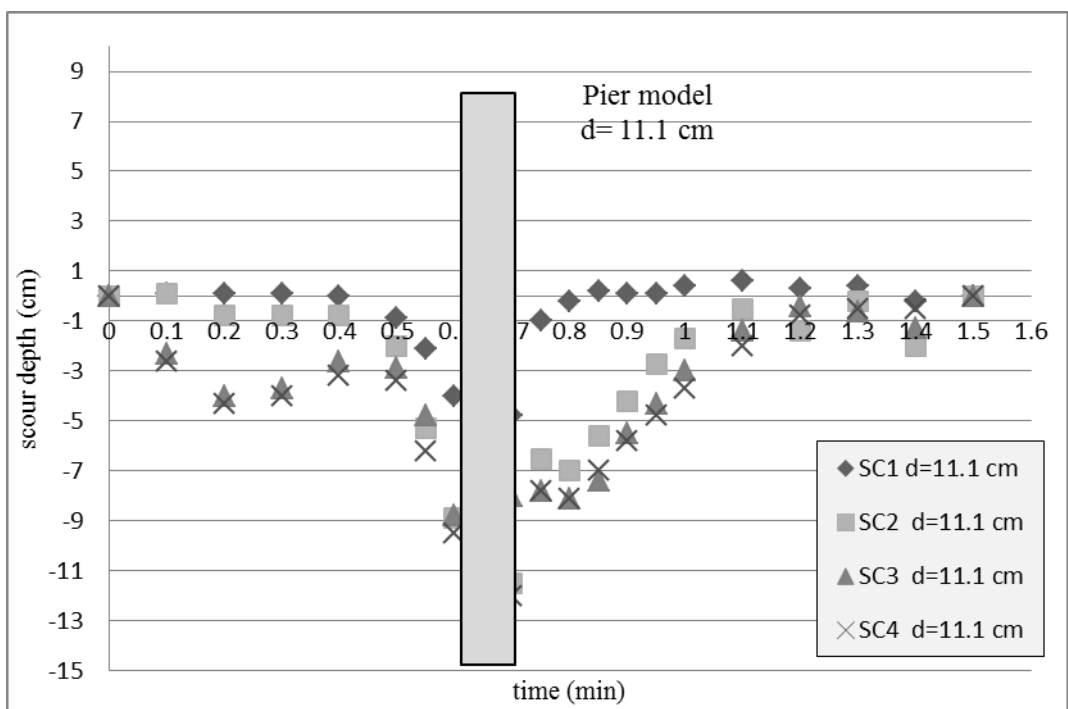


Figure 4.37 Longitudinal scour profiles for Group 3

4.5 Predicting maximum scour depth

In this study there are parameters effects on maximum scour depth; results of three Group tests show us the relation between these parameters and maximum scour depth. Computer software Step-wise Regression© which it was one of the regression analysis methods and fitted data, Step-wise Regression used in this study to analyses the results of the maximum scour depth to get formula which give us maximum scour depth (d_s).The parameters like (d) pier width, (t) time of equilibrium, (Q) discharge, (h) flow depth, used to analyses a formula for maximum scour depth. In the program, there are many types of regression method as shown in Figure 4.38, it will necessary to try all methods to know the best one. In this study, linear method, linear+ interaction method, and full quadratic method are used to predict maximum scour depth, it is seen that the last method is the best method in this study to predict maximum scour depth.

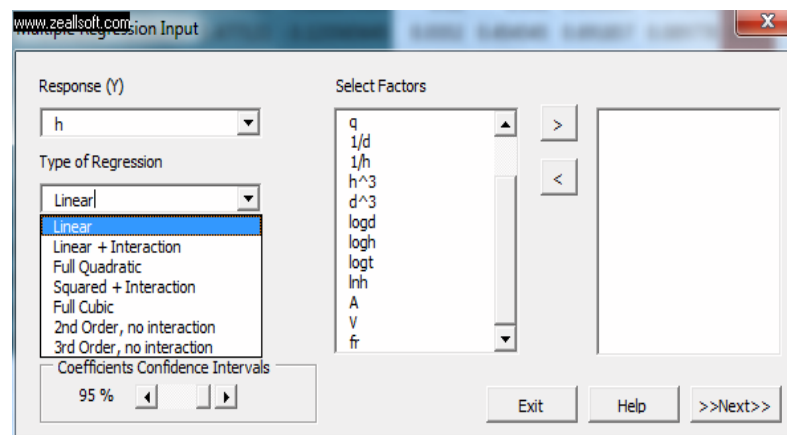


Figure 4.38 Step-wise regression input window.

4.5.1 Linear Regression Method

This is the simplest method to get the formule in step-wise program, the results of this method was shown in Equation 4.1with R-square value of $R^2 = 0.943$, and with Standard Error of 0.00637, as shown in (Table 4.13).

$$dse = 0.664 + 0.103 * \ln h - 0.216 * u - 0.0327 * \log t + 0.0897 * \log d \quad (4.1)$$

Where h: depth flow (m) u: approach velocity (m²/s) t: time of equilibrium (min) d: pier diameter (m). Figure 4.44 shows the comparison between determined maximum scour depths from linear equation and observed from experimental work.

Table 4.13 Summary of linear method

R	0.971
R ²	0.943
R ² adjusted	0.910
Standard Error	0.00638
# Points	12
PRESS	0.00
R ² for Prediction	0.453
Durbin-Watson d	2.684
First Order Autocorrelation	-0.405
Collinearity	0.012
Coefficient of Variation	7.153

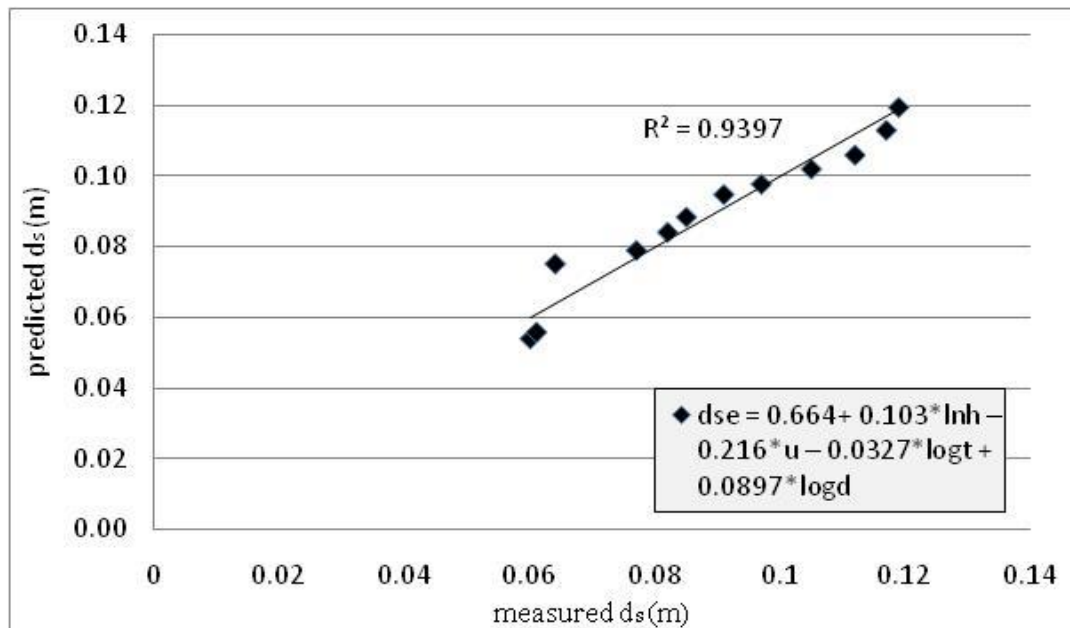


Figure 4.39 Comparison of the measured sc scour depth d_s with the predicted one by linear regression.

4.5.2 Linear + Interaction Method

The formule results acording to linear+intraction method depending on, (h) depth flow, (d) pier diameter, and (Q) discharge of flow, with R-square value $R^2= 0.986$ and Standard Error of 0.00298The summary are shown in Table 4.14.Figure 4.45 shows the comparison between determined and observed maximum scour depths using linear+interaction equation. The following equation is formed as.

$$d_{se} = - 0.118 + 18.681 h * d^2 - 21.241 Q * d^2 + 0.0504 \log d * \log h \quad (4.2)$$

Where

d_{se} : Equilibrium scour depth (m)

h : Flow depth (m)

d : Pier diameter (m)

Q : Flow discharge (m^3/s)

Table 4.14. Summary of linear+ interaction method

R	0.993
R^2	0.986
R^2 adjusted	0.980
Standard Error	0.00299
# Points	12
PRESS	0.00
R^2 for Prediction	0.953
Durbin-Watson d	2.112
First Order Autocorrelation	-0.287
Collinearity	0.001
Coefficient of Variation	3.353

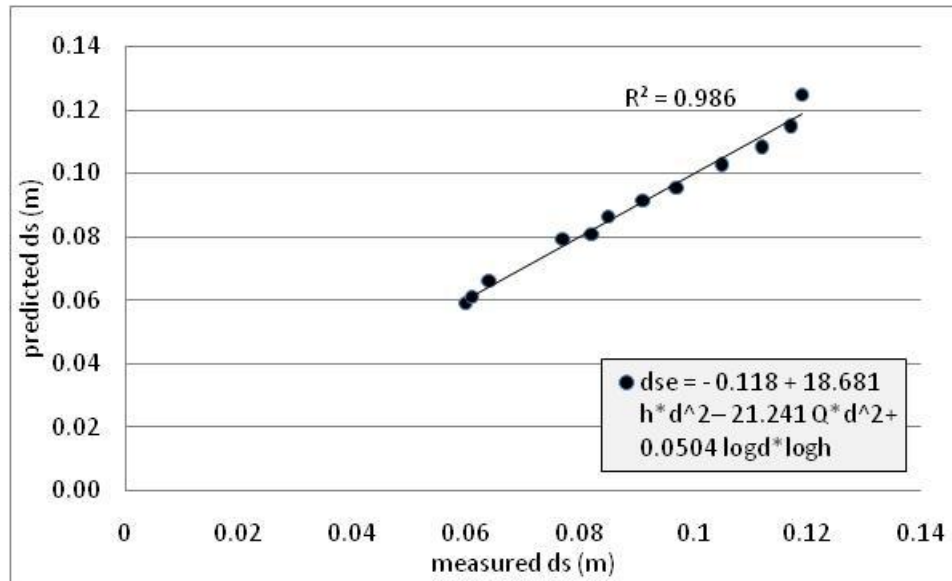


Figure 4.40 Comparison of the measured scour depth d_s with the predicted one by linear+interaction regression.

4.5.3 Quadratic Regression Method

The formule results acoording to this method depending on, (h) depth flow, (d) pier diameter, (Q) discharge, with R- square value $R^2= 0.988$ and Standard Error of 0.00260 the summary are shown in Table 4.15. According to this results the quadratic method was an best suited method to predict equilibrium scour depth by Equation 4.3 for this study. Figure 4.46, shows the comparison between determined and observed maximum scour depths using quadratic equation.

$$d_{se} = 0.0548 - 0.0427 d * \frac{1}{h} - 0.351 d * \ln Q \quad (4.3)$$

Where d_{se} : Equilibrium scour depth (m), d: Pier diameter (m), Q: Flow discharge (m^3/s)

Table 4.15 Summary of quadratic method

R	0.994
R ²	0.988
R ² adjusted	0.985
Standard Error	0.00261
# Points	12
PRESS	0.00
R ² for Prediction	0.983
Durbin-Watson d	1.976
First Order Autocorrelation	-0.007
Collinearity	0.231
Coefficient of Variation	2.925

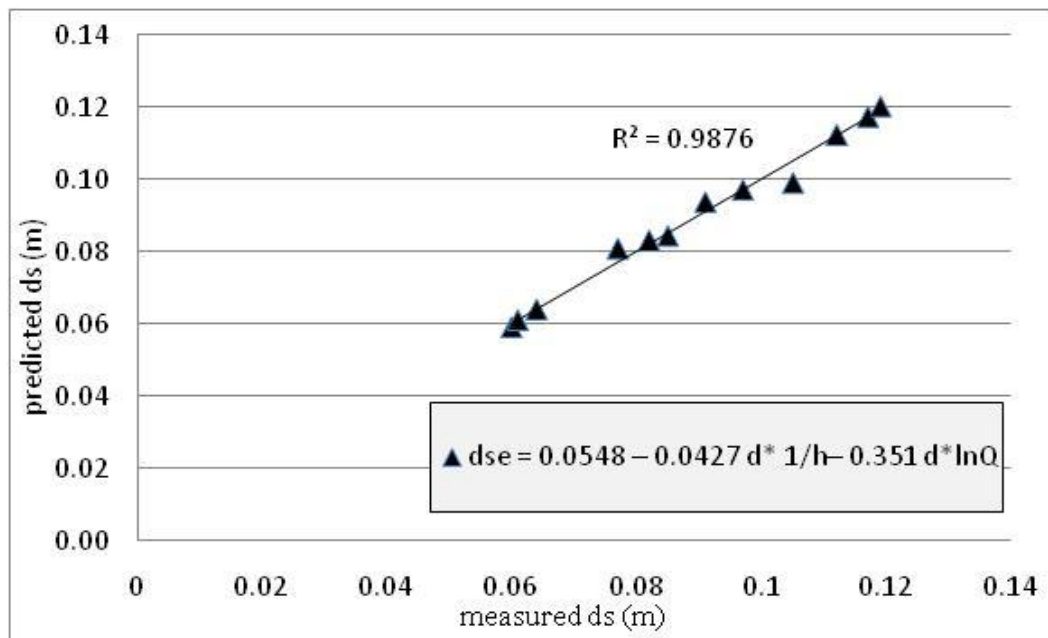


Figure 4.41 Comparison of the measured scour depth d_s with the predicted one by Quadratic regression

Table 4.16 shows the maximum scour depth which determined from experimental work and maximum scour depth for the predicted equations from the three methods as shown. The mean and standard deviation for each method was calculated and given in the following table, it's clear from results that the quadratic method found as the best method in this study. The input data for the program are shown in Appendix B.

Table 4.16 Comparison of three regression methods

measured d_{sc}	(4.1) eq.	$d_{sc}/(4.1)$ eq.	(4.2) eq.	$d_{sc}/(4.2)$ eq.	(4.3) eq.	$d_{sc}/(4.3)$ eq.
0.06	0.054	1.110	0.059	1.014	0.058	1.019
0.077	0.079	0.974	0.079	0.971	0.080	0.954
0.082	0.084	0.974	0.080	1.016	0.082	0.989
0.085	0.088	0.960	0.086	0.985	0.084	1.009
0.061	0.055	1.091	0.060	1.000	0.060	1.001
0.091	0.094	0.959	0.091	0.995	0.093	0.972
0.097	0.097	0.992	0.095	1.017	0.096	1.000
0.105	0.102	1.028	0.103	1.021	0.098	1.062
0.064	0.075	0.850	0.066	0.966	0.063	1.002
0.112	0.106	1.056	0.108	1.033	0.112	0.998
0.117	0.113	1.035	0.115	1.017	0.117	0.998
0.119	0.120	0.995	0.125	0.954	0.120	0.991
0.06	Mean	1.00253		0.99964		1.0001
	Standard deviation	0.06920		0.02505		0.02574

CHAPTER 5

CONCLUSIONS

5.1 Conclusion

In this thesis, temporal development and equilibrium maximum scour depth was studied in Gaziantep University, Hydraulic Laboratory by using three samples of cylindrical bridge piers with different diameters tested with four different discharges to show how the pier diameter effect on local scour and then analysis the results to predict a maximum scour equation by using computer software Step-Wise regression. The following conclusions are made from this study:

1. In this thesis, the present experimental results show that there is a relation between depth of scour and pier diameter where the depth of scour increases with increase pier diameter for the same sediments size and discharge.
2. Our experimental study also show that there is a relation between the size of the sediments and maximum scour depth with decreasing the mean size of the sediments the maximum scour depth increases.
3. The deposition is not occurred at high discharges. Scour is occurring as live bed scour.
4. During experimental work when started the test, observed that scour depth increase suddenly in 10 or 15 minutes, after this time scour depth develops reached to equilibrium state.

5. The experimental result shows that, when increase the discharge the scour depth increase with fixed pier diameter.

5.2 Recommendation for future study

1. In this work, the researcher formulates relation between pier diameter, discharge, and scour depth with fixed median particle size of sand (d_{50}). The relation may be developed in future to include median particle size (d_{50}) to study how its effect to scour depth.
2. The cylindrical bridge pier was used in this work to study the temporal development of scour depth around it. But different pier shapes should be used in the experiments to find out best pier shape.
3. In future it can be possible to use one of the simulation programs like FLUENT which apply computer simulation methods to analyze and solve practical design problems based on fundamental principles of Computational Fluid Dynamics (CFD), to simulate scour depth and modeling fluid flow around the bridge pier.

REFERENCES

Breusers, H.N.C., Nicollet, G. and Shen, H.W."Local scour around cylindrical piers". (1977) *Journal of Hydraulic Research*, **15(3)**: 211-252.

Breusers, H. N. C. (1965). "Scour around drilling platforms." *International Association of Hydraulic Research*.

Breusers, H.N.C. and Raudkivi, A.J. (1991). Scouring - Hydraulic structures design manual. IAHR, A.A. *Balkema, Rotterdam*, 143 p.

Dargahi, B. (1982) "The Turbulent Flow Field around a Circular Cylinder", *Experiments in Fluids*, **vol.8**, pp.1-12.

Dey, S., Bose, S.K., and Sastry, G.L.N., (1995), "Clear Water Scour at Circular Piers: A Model." *Journal of Hydraulic Engineering*, **Vol.121**, No. 12, pp. 869-876.

Ettema, R. (1980). Scour at bridge piers. PhD Thesis, *Auckland University, Auckland, New Zealand*.

Graf, W.H, and Istiarto, I, (2001), "Flow Pattern in the Scour Hole around a Cylinder." *Journal of Hydraulic Research*, **Vol. 40**, No. 1, pp. 13-20

Graf, W.H, and Istiarto, I, (2001), "Flow Pattern in the Scour Hole around a Cylinder." *Journal of Hydraulic Research*, **Vol. 40**, No. 1, pp. 13-20

Hosny M. M. (1995) "Experimental Study of Local Scour around Circular Bridge Piers in Cohesive Soils". Ph.D. Dissertation, Civil Engineering Department, Colorado State University, *Fort Collins, Colorado, USA*.

Hoffmans, G.J.C.M. and Verheij, H.J. (1997). Scour manual. *A.A. Balkema, Rotterdam, Netherlands*, 205 p.

Laursen, E.M., (1963), "An Analysis of Relief Bridge Scour." *Journal of Hydraulics Division, ASCE*, **Vol. 89**, No. HY3, pp. 93-118.

Laursen, E.M., and Toch, A. (1956) "Scour around bridge piers and abutments", *Bull. No. 4, Iowa Hwy. Res. Board, Ames, Iowa*.

Melville, B.W. and Raudkivi, A.J. "Flow characteristics in local scour at bridge piers". *Journal of Hydraulic Research*.(1977) IAHR, **15(1)**:373-380.

Melville, B., Sutherland, A.J. (1988). Design Method for Local Scour at Bridge Piers, *Journal of Hydraulic Engineering*, **114 (10)**, 1210-1226.

Melville, B.W. and Coleman, S.E. (2000). Bridge scour. *Water Resources Publications, LLC, Colorado, U.S.A.*, 550 p.

Melville, B.W. and Chiew, Y.M. (1999). Time scale for local scour at bridge piers,

“Journal of Hydraulic Engineering”, ASCE, **125(1)**: 59-65.

Ming Zhao, and Liang Cheng (2010), “Experimental and numerical investigation of local scour around a submerged vertical circular cylinder in steady currents” *journal of sinedirect, Coastal Engineering*, **Vo.157** (2010) 709–721.

Mia, M. F., and Nago, H. (2003). “Design method of time-dependent local scour at circular bridge pier.” *J. Hydraul. Eng.*, **Vol.129_6_**, 420– 427.

McIntosh, J.L., (1989), Use of scour prediction formulae, Proceedings of the Bridge Scour Symposium: McLean, VA, *Federal Highway Administration Research Report FHWA-RD-90-035 LLC*, (2000) Colorado, U.S.A., 550 p.

Richardson, E.V., Harrison, L.J., Richardson, J.R., and Davis, S.R., (1993), Evaluating scour at bridges: Federal *Highway Administration Hydraulic Engineering Circular No. 18 (HEC-18)*, Publication No. FHWA-IP-90-017, 132 p.

Richardson, E.V., and Davis, S.R., 2001, “Evaluating Scour at Bridges (4th ed.)”, *Federal Highway Administration Hydraulic Engineering Circular .No. 18*, FHWA NHI 01-001.

Shen, H.W., Schneider, V.R. and Karaki, S.S., (1966), "Mechanics of Local Scour", *Colorado State University, Civil Engineering Dept., Fort Collins, Colorado*, Pub. No. CER66-HWS22.

Shen, H.W., Schneider, V.R. and Karaki, S., (1969), “Local scour around bridge”,

Proceedings ASCE, Journal of Hydraulics Div., Vol. 95, No. HY6, pp 1919-1940.

Dr Les Hamill , (1999), " Bridge Hydraulic Theory and Practice ": *first published, by E & FN spon*, pp. 347-348.

Yanmaz, A.M., Altinbilek, H.D. (1991), "Study of Time-Dependent Local Scour around Bridge Piers", *J. Hydraulic Engineering. Vol. 117*, No.10, pp.1247-1268

<http://en.wikipedia.org/wiki/Vortex>, 02/9/2012.

APPENDIX A

Table A. Data for scour profile

		SA1	SA2	SA3	SA4	SB1	SB2	SB3	SC4	SC1	SC2	SC3	SB4
X	Y	Z	Z	Z	Z	Z	Z	Z	Z	Z	Z	Z	Z
0	0	20	20	20	20	20	20	20	20	20	20	20	20
10	0	20	20	20	20	20	20	20	20	20	20	20	20
20	0	20	20	20	20	20	20	20	20	20	20	20	20
30	0	20	20	20	20	20	20	20	20	20	20	20	20
40	0	20	20	20	20	20	20	20	20	20	20	20	20
50	0	20	20	20	20	20	20	20	20	20	20	20	20
60	0	20	20	20	20	20	20	20	20	20	20	20	20
70	0	20	20	20	20	20	20	20	20	20	20	20	20
80	0	20	20	20	20	20	20	20	20	20	20	20	20
90	0	20	20	20	20	20	20	20	20	20	20	20	20
100	0	20	20	20	20	20	20	20	20	20	20	20	20
110	0	20	20	20	20	20	20	20	20	20	20	20	20
120	0	20	20	20	20	20	20	20	20	20	20	20	20
130	0	20	20	20	20	20	20	20	20	20	20	20	20
140	0	20	20	20	20	20	20	20	20	20	20	20	20
150	0	20	20	20	20	20	20	20	20	20	20	20	20
0	10	20	20	20	20	20	20	20	20	20	20	20	20
10	10	19	17.7	17.3	17.6	19.1	17.9	17.9	17.6	19.2	17.8	17.6	17.6
20	10	20	17.2	15.7	15.6	20	17.2	16	15.5	20.1	17.5	16	15.5
30	10	20	18.2	16.5	15.6	19.2	18.5	17	15.8	19.6	18.8	16.4	15.8
40	10	19.7	18.8	17.5	16.9	19.8	19.2	18	17.4	20	19.1	17.7	17.4
50	10	19.7	19.1	18	17.6	19.6	19.4	18.1	18	19.8	19.3	18.1	18
60	10	19.4	19.2	18.5	17.4	19.9	19.5	18.3	18.4	20	19.3	18.6	18.4
70	10	19.6	19.9	18.5	18.2	19.9	19.8	18.5	18.8	19.7	19.5	18.9	18.8
80	10	19.8	18.8	18.5	18.3	19	19.8	18.5	18.8	19.9	19.2	19	18.8
90	10	19.5	18.6	18.5	18.4	17.2	19.5	18.2	18.5	19.2	18.2	18.6	18.5
100	10	19.3	18.5	18.4	18.2	19	19	18.3	18.2	19.2	18	18.3	18.2
110	10	19.1	18.4	18.3	18.3	19	18.7	18.1	17.5	16.8	18.4	18.2	17.5
120	10	18.9	18.4	18.2	18.1	19.1	18	18	17.3	17	17	17.5	17.3
130	10	18.4	18	18	18	19.3	18	18	16.7	18.1	18	17	16.7
140	10	19	18.2	17.8	19	19.2	17.5	18.4	17	18.5	17.1	17.1	17
150	10	17.5	18	18.3	19	17	16	16.8	16	15.8	14	14	16
0	20	20	20	20	20	20	20	20	20	20	20	20	20
10	20	19.3	17.6	17.6	17.7	19.3	17.9	17.7	18	19.1	17.8	17.7	17.5
20	20	20.3	17	16.1	15.9	19.8	17.3	15.8	15.8	20.2	17.6	16.2	16
30	20	20	18	16.5	15.8	19.5	18.5	16	15.2	19.5	18.8	16.3	16
40	20	19.7	18.5	17.7	16.9	20	18.9	17.3	15.9	19.9	18.8	17.5	17.2
50	20	19.9	18.6	18.2	17.7	19	19.2	18	17	19.3	18.8	17.9	17.5

60	20	19.8	18.8	18.3	18	19	19.5	18.3	17.2	20	18.5	17.9	17.8
70	20	19.6	19.1	18.5	18	19.9	19.8	18.4	17.7	19.7	17	16.7	16.5
80	20	19.4	19.1	18.6	17.9	19	19.5	18.2	16.4	19.6	17.5	16.9	16.8
90	20	18.3	18.7	18.4	17.9	18.3	19	18	17.1	20	18.1	17.4	17.3
100	20	19.5	18.7	18.3	17.6	19.6	18.5	18	17	19.3	18	17.7	17.5
110	20	18.5	18.3	18.1	17.7	19.2	18	17.7	17.5	19.9	17.8	17.2	17.5
120	20	18.8	18.4	18	17.9	20	17.9	17.6	17.5	18.5	17.3	17.1	16.8
130	20	18.2	18.2	17.8	18	19.9	17.4	18	17.6	19.5	18.1	17.2	17.3
140	20	17.9	18.2	17.9	19	19.2	18	18.3	17.5	18.7	16.8	17.8	18
150	20	19	18.9	18.6	19	18.9	17.2	15.3	16.5	18.3	15.6	14	16
50	25	20	18.8	18	17.6	18.8	19.1	18	17	20	18.6	17.8	17.3
55	25	19.9	18.9	18.9	17.7	19.5	19.1	18	17.1	18.9	17.4	17.6	17.1
60	25	20	18.9	18.3	18.1	19.7	19	17.9	17.2	18.9	15.2	16.1	15.5
65	25	20	19	18.2	18.2	19	18	17.2	17.1	18.2	13.9	14.1	14
70	25	20	18.7	18	18.1	18.5	17	16.5	16.1	18.5	13.8	13.5	13.6
75	25	19.7	18.6	17.9	17.8	19	17.3	16.5	16	18.1	14.3	13.8	14
80	25	19.6	18.5	17.8	17.7	19.3	17.7	16.9	16.3	19.2	15.8	15.3	15.1
85	25	19.4	18.5	17.9	17.8	19.8	18	17	16.6	20.1	16.5	16.4	16.1
90	25	19.2	18.3	17.8	17.9	20	18	17.3	17	20.2	16.7	16.9	16.5
95	25	19	18.1	17.8	17.9	20	18	17.4	16.3	19.7	17	17.3	17
0	30	20	20	20	20	20	20	20	20	20	20	20	20
10	30	20	17.5	17.5	17.5	19.9	17.9	17.9	17.5	19.9	18	17.7	17.5
20	30	20.2	17.1	16	15.9	20	17.4	16	15.7	20.6	17.7	16.2	16
30	30	20.8	18.6	16.5	15.9	19.9	18.5	16.4	15.2	19.9	18.6	16.5	16
40	30	20	18.7	17.6	17	19.6	18.9	17.5	16.3	20.1	18.6	17.5	16.9
50	30	20.1	18.8	18.1	17.6	18.5	19	17.9	17	19.9	18.3	17.5	17
55	30	20.2	18.6	18.1	17.7	18	19	17.7	17	19.6	16	16.5	16.2
60	30	20	18.5	17.6	17.7	17.7	16.7	16.2	16.3	18	13.5	14.4	13.4
65	30	18.8	16.7	16	16.4	17.5	15	14.4	14	16.7	12	11.7	11.3
70	30	18.4	16.2	15.5	15.7	17.5	14.5	15.7	13	16.4	11.4	10.5	10.5
75	30	18.8	16.4	15.8	16.3	19	15.2	14.5	13.8	18.9	12.2	11.1	11
80	30	19	16.8	16.4	16.8	19.8	16.2	15.6	14.8	19	13.5	12.7	12.6
85	30	18.8	17.2	16.9	17	19.8	16.8	16.4	15.8	19	14.9	14.6	14.1
90	30	18.6	17.2	17	17.2	20	17.2	16.8	16.5	19.8	15.9	15.6	15.3
95	30	18.6	17.3	17.2	17.4	20	17.3	17	16.7	20.4	16.5	16.6	15.9
100	30	19	18	17.3	17.6	19.5	17.5	17.1	17	20.1	16.9	17	16.3
110	30	19.8	18.2	17.8	18	20.4	18.2	17.4	17.5	20.8	17.9	17.4	16.9
120	30	20	18.8	18.1	18.2	20.7	19.2	18	17.5	20.5	18.7	18.5	17.7
130	30	18.8	18.9	18.3	18.5	20.2	19.5	18.6	18	20.3	19.3	18.7	18.2
140	30	19.8	19.1	18.5	18.5	19	19.8	18.8	18.5	19.7	19.6	18.6	18.6
150	30	17.4	19.2	19.3	19.2	18.5	17.5	19.3	17.5	18.8	16.7	17.8	17.2
50	35	20.1	18.5	18	17.5	18.5	18.7	17.9	17	19.3	17.5	17.5	16.9
55	35	20.1	18.4	17.9	17.5	19.1	18.1	17.4	16.9	17.8	14.3	15.5	14.7
60	35	19	16.6	16	15.6	17.8	15.6	14.3	14.3	16.4	11.9	12	11.6
65	35	16.4	14.3	13.5	13	15.2	13	11.5	11.5	14.2	9.2	8.4	8.6

70	35	15.3	13.8	13.3	13	15.3	11.6	11	10.5	15.1	10.1	9	9
75	35	16.8	15.2	14.8	15	16.4	12.5	12.3	11.5	16.3	11.4	10.9	10.2
80	35	17.8	16	15.9	16	18	14.6	14.1	13.5	18.1	12.8	11.5	11.1
85	35	18.5	16.9	16.7	16.3	19	16.2	15.4	15.1	18.5	14.4	13.6	12.6
90	35	19.4	17.3	17	17.2	20.3	16.9	16.3	16.5	19.2	15.6	15.1	14
95	35	20.1	17.7	17.2	17.6	20.2	17.6	16.8	17	20.4	16.8	16.3	15
0	40	20	20	20	20	20	20	20	20	20	20	20	20
10	40	20	17.4	17.3	17.7	19.9	17.9	17.5	17.5	20.1	20.1	17.7	17.4
20	40	20	17.1	15.7	15.6	20	17.5	16	15.6	20.1	19.2	16	15.7
30	40	20.2	18.5	16.3	15.9	19.9	18.6	16.5	15.2	20.1	19.2	16.3	16
40	40	19.9	18.7	17.4	17	19.6	19	17.3	16.1	20	19.2	17.4	16.8
50	40	19.8	18.5	17.7	17.5	18.5	18.7	17.9	17	19.1	18	17.1	16.6
55	40	19.9	18.4	17.7	17.5	19.1	17.9	16.5	16.7	18.9	14.7	15.2	13.8
60	40	18.7	16.7	14.6	16	17.8	14.4	15.7	13.5	16	11.1	11.2	10.5
65	40	14	12.3	12.9	11.5	13.9	10.9	10.3	9.5	13.8	8.8	8.3	8.1
70	40	16.2	13.8	13.4	13.3	13.9	10.9	10.3	9.5	13.8	8.8	8.3	8.1
75	40	16.6	14.4	14.2	13.5	17.3	13.5	12.7	12	19	15.5	12.2	12.2
80	40	18.5	15.8	16	15.2	18.2	14.4	14	13	19.8	13	11.9	12
85	40	20	17.5	17.4	17	19.5	16.4	15.5	14.4	20.2	14.4	12.6	13
90	40	20.4	18.7	18.4	18.1	20.5	18	16.9	16	20.2	15.8	14.5	14.2
95	40	20.7	19.2	18.9	18.6	20.2	19.1	18	17.1	20.1	17.3	15.7	15.2
100	40	20.8	19.7	19.1	19.1	20.7	20	18.8	18.2	20.4	18.3	17	16.3
110	40	20.6	19.5	19.6	19.6	20.4	19.5	19.6	19.3	20.6	19.5	18.6	18
120	40	20.2	19.6	19.6	19.8	20.7	19.7	19.9	19.7	20.3	18.6	19.6	19.2
130	40	17.7	19.4	19.3	19.6	20.2	19.8	19.8	19	20.4	19.8	19.4	19.5
140	40	18.3	19.4	18.8	19.2	20	20	19	18.5	19.8	18	18.7	19.5
150	40	17.5	19	18.5	19.1	18.5	18.5	19	18	19.1	19.7	18.3	19.1
50	45	19.9	18.5	17.8	17.6	18.5	18.8	17.8	16.9	19.1	18	17.1	16.5
55	45	19.9	18.5	17.7	17.5	18	18	17.5	16.9	18	14.8	15.1	14
60	45	19	17.4	16.4	16	17.7	15.1	14.5	14	16.7	11.7	11.8	11
65	45	16.7	14.9	14.2	13.4	15.3	12.3	12.1	10.5	14.3	9.4	8.6	8.5
70	45	16	14	13.7	13.6	15.3	11.6	10.7	10.4	15.1	10.2	9	8.8
75	45	17.2	15.8	15	14.9	16.4	12.7	12	11.3	16.1	11.4	10.9	10
80	45	18.2	16.7	16	15.9	18	14.9	14.8	13.5	18.4	12.6	11.5	12
85	45	18.8	17.3	16.7	16.6	19	16.5	16	15	18.5	15.8	13.5	14.3
90	45	19.3	17.9	17.3	17.2	20	17.5	16.9	15.7	19.2	15	15.1	15.9
95	45	19.4	18.3	17.8	17.6	20	18	17.5	16.9	20.3	16.3	16	16.9
0	50	20	20	20	20	20	20	20	20	20	20	20	20
10	50	19.7	17.6	17.6	17.7	19.3	17.9	17.8	17.6	20	17.7	17.5	13.3
20	50	20	16.9	15.7	15.7	20.2	17.3	15.9	15.6	19.9	17.3	16	15.4
30	50	20	18	16.2	15.9	19.5	17.5	16.3	15.2	20.1	18.5	16.4	15.7
40	50	19.9	18.5	17.3	17	20	18.9	17.4	16	20.1	18.9	17.5	16.5
50	50	19.8	18.6	17.9	17.6	18.8	18.9	17.9	17	19.4	18.9	17.2	16.8
55	50	19.8	18.6	17.9	17.6	19.5	18.8	17.7	17.2	18.8	16.1	15.8	15.4
60	50	19.8	18.5	17.7	17.6	19.7	16.7	16.5	15.7	17.4	13.8	13.3	12.9

65	50	19.2	17.8	16.5	16.8	17.5	15	14.3	13.7	17	12	11.3	10.8
70	50	18.8	16.8	16.1	16	17.5	14.4	13.5	13	17	11.4	10.7	10.2
75	50	18.8	16.7	16.1	16.2	19	15.2	14.3	14	18.5	12.4	11.4	11.3
80	50	18.8	17.1	16.4	16.5	19.8	16.3	15.4	15.4	19.1	13.7	13.3	13.3
85	50	18.3	17.4	16.9	16.9	18.7	17	16.3	16.3	18.6	15.1	15.1	15.2
90	50	18.9	17.6	17.3	17.1	20	17.4	16.8	16.5	19.2	16	16.2	16.2
95	50	19	17.7	17.5	17.4	20	17.6	17.1	16.7	19	16.1	16.4	16.9
100	50	18.5	17.9	17.7	17.6	19.5	17.7	17.3	16.9	19.7	16.7	17.6	17.3
110	50	17	18.3	18.2	18	20.4	18.5	17.9	17	20.7	18	17.7	18
120	50	18.9	18.8	18.7	18.3	20	19.4	18.5	17.7	21	19.8	18.7	18.4
130	50	20	19	18.9	18.6	19.9	19.5	19.1	18.2	20.8	20.3	18.8	18.4
140	50	18.8	19.1	18.8	18.2	19	19.8	19.3	18.7	19.8	20	18.8	18.5
150	50	18.5	19.1	19.1	19.2	18.9	19.3	18.5	19	19.3	17.6	15	18.4
50	55	19.8	18.8	18	17.6	19	19	18.1	17	19.5	19	17.5	17
55	55	20	18.8	18.1	17.8	19.5	19	18.1	17.3	19.3	18.3	17.4	17
60	55	19.7	19	18.2	17.9	19	18.8	18.1	17.3	18.7	16.1	15.5	15.5
65	55	19.1	19.1	18.3	18	19	17.8	17.2	16.4	18.4	14.7	14.1	14
70	55	19.3	19.1	18.3	18.1	18.5	17.3	16.4	15.9	18.3	14.4	13.7	13.6
75	55	19.3	19	18.4	18	19	17.5	16.5	16	18.8	15.3	14.3	14.2
80	55	19	18.7	18.2	17.9	19.3	17.7	16.8	16.4	19.4	16.5	15.5	15.3
85	55	19	18.7	18	17.9	18.7	18	17.1	16.8	19.5	17.2	16.4	16.3
90	55	18.2	18.7	18	17.9	18.3	18	17.3	16.9	19.5	17.1	16.9	16.9
95	55	18	18.4	18	17.8	19	18	17.4	16.9	19.1	17	17.6	17
0	60	20	20	20	20	20	20	20	20	20	20	20	20
10	60	20	17.6	17.3	17.6	19.1	17.8	17.6	17.7	20	17.8	17.5	17.3
20	60	20	16.9	15.7	15.6	20	17.2	15.6	15.7	20.1	16.9	16	15.5
30	60	19.6	16.9	15.9	15.5	19.2	18.4	15.9	15	20.1	18.3	16.1	15.2
40	60	17.2	18.8	17.3	16.6	19.8	19	17.3	15.9	20	18.8	17.4	16.2
50	60	17	18.9	18.1	17.5	19.6	19.1	18.1	17	19.9	19.5	17.6	17.2
60	60	19.6	19	18.5	18	19.9	19.4	18.3	17.5	19.4	19.5	17.8	17.5
70	60	19	19.2	18.5	18.3	19.9	19.4	18.4	17.7	19.3	17.6	16.8	16.9
80	60	18.7	19.1	18.9	18.5	19	19	18.2	17.7	19.6	18.2	16.8	17.1
90	60	18.7	18.7	18.7	18.4	17.2	18.5	18.1	17.4	19.5	18.7	17.1	17.5
100	60	18.7	18.7	18.4	18.2	19.6	18.4	17.9	17.4	18.9	17.5	17.3	17.5
110	60	18.6	18.3	18.2	18	19	18	17.7	17.1	18.8	17.2	17.5	17.3
120	60	18.8	18.4	18	18	19.1	17.9	17.6	17	18.7	17.4	17.5	17.2
130	60	20	18.2	18.2	18	19.3	17.7	18	17.7	18.5	18.1	17	17.7
140	60	20.3	18.2	17.8	18	19.2	19	18.3	18	19	17.5	17.2	17.9
150	60	19	18.9	18.8	18.7	17	15	15	15.5	17.4	14	13	16
0	70	20	20	20	20	20	20	20	20	20	20	20	20
10	70	20	20	20	20	20	20	20	20	20	20	20	20
20	70	20	20	20	20	20	20	20	20	20	20	20	20
30	70	20	20	20	20	20	20	20	20	20	20	20	20
40	70	20	20	20	20	20	20	20	20	20	20	20	20
50	70	20	20	20	20	20	20	20	20	20	20	20	20

60	70	20	20	20	20	20	20	20	20	20	20	20	20
70	70	20	20	20	20	20	20	20	20	20	20	20	20
80	70	20	20	20	20	20	20	20	20	20	20	20	20
90	70	20	20	20	20	20	20	20	20	20	20	20	20
100	70	20	20	20	20	20	20	20	20	20	20	20	20
110	70	20	20	20	20	20	20	20	20	20	20	20	20
120	70	20	20	20	20	20	20	20	20	20	20	20	20
130	70	20	20	20	20	20	20	20	20	20	20	20	20
140	70	20	20	20	20	20	20	20	20	20	20	20	20
150	70	20	20	20	20	20	20	20	20	20	20	20	20
0	80	20	20	20	20	20	20	20	20	20	20	20	20
10	80	20	20	20	20	20	20	20	20	20	20	20	20
20	80	20	20	20	20	20	20	20	20	20	20	20	20
30	80	20	20	20	20	20	20	20	20	20	20	20	20
40	80	20	20	20	20	20	20	20	20	20	20	20	20
50	80	20	20	20	20	20	20	20	20	20	20	20	20
60	80	20	20	20	20	20	20	20	20	20	20	20	20
70	80	20	20	20	20	20	20	20	20	20	20	20	20
80	80	20	20	20	20	20	20	20	20	20	20	20	20
90	80	20	20	20	20	20	20	20	20	20	20	20	20
100	80	20	20	20	20	20	20	20	20	20	20	20	20
110	80	20	20	20	20	20	20	20	20	20	20	20	20
120	80	20	20	20	20	20	20	20	20	20	20	20	20
130	80	20	20	20	20	20	20	20	20	20	20	20	20
140	80	20	20	20	20	20	20	20	20	20	20	20	20
150	80	20	20	20	20	20	20	20	20	20	20	20	20

APPENDIX B

Table B. Input data in step- wise program

d(cm)	h(m)	t(min)	q(m ³ /s)	1/d	1/h	logd	logh	logt	lnh	a(m ²)	v(m ² /s)	d ²	ln q	ln d
5	0.025	15	0.00692	20	40	-1.301	-1.602	1.1760	-3.688	0.02	0.346	0.2236	-4.97333	-2.9957
5	0.044	30	0.016	20	22.72	-1.301	-1.356	1.4771	-3.123	0.0352	0.4545	0.2236	-4.13516	-2.9957
5	0.054	30	0.02263	20	18.51	-1.301	-1.267	1.4771	-2.918	0.044	0.5286	0.2236	-3.76102	-2.9957
5	0.058	30	0.02519	20	17.24	-1.301	-1.236	1.4771	-2.847	0.0464	0.5428	0.2236	-3.68130	-2.9957
7.5	0.025	40	0.00692	13.33	40	-1.124	-1.602	1.602	-3.688	0.02	0.34	0.2738	-4.97333	-2.5902
7.5	0.044	30	0.016	13.33	22.72	-1.124	-1.356	1.4771	-3.123	0.0352	0.4545	0.2738	-4.13516	-2.5902
7.5	0.054	35	0.02263	13.33	18.51	-1.124	-1.267	1.5440	-2.9187	0.044	0.528636	0.2738	-3.76102	-2.5902
7.5	0.058	35	0.02519	13.33	17.24	-1.124	-1.236	1.5440	-2.8473	0.0464	0.542888	0.2738	-3.68130	-2.5902
11.1	0.025	30	0.00692	9.009	40	-0.954	-1.602	1.4771	-3.6888	0.02	0.346	0.3331	-4.97333	-2.1982
11.1	0.044	40	0.016	9.009	22.72	-0.954	-1.356	1.602	-3.1235	0.0352	0.454545	0.3331	-4.13516	-2.1982
11.1	0.054	35	0.02263	9.009	18.51	-0.954	-1.267	1.5440	-2.9187	0.044	0.528636	0.3331	-3.76102	-2.1982
11.1	0.058	30	0.02519	9.009	17.24	-0.954	-1.236	1.4771	-2.8473	0.0464	0.542888	0.3331	-3.68130	-2.1982